LAWRENCE
LIVERMORE
NATIONAL
LABORATORY

LLNL-JRNL-424225

Structure of the Crust beneath Cameroon, West Africa, from the Joint Inversion of Rayleigh Wave Group Velocities and Receiver Functions

A.-P. K. Tokam, C.T. Tabod, A.A. Nyblade, J. Julia, D.A. Wiens, M.E. Pasyanos

February 22, 2010

Geophysical Journal International

Disclaimer

This document was prepared as an account of work sponsored by an agency of the United States government. Neither the United States government nor Lawrence Livermore National Security, LLC, nor any of their employees makes any warranty, expressed or implied, or assumes any legal liability or responsibility for the accuracy, completeness, or usefulness of any information, apparatus, product, or process disclosed, or represents that its use would not infringe privately owned rights. Reference herein to any specific commercial product, process, or service by trade name, trademark, manufacturer, or otherwise does not necessarily constitute or imply its endorsement, recommendation, or favoring by the United States government or Lawrence Livermore National Security, LLC. The views and opinions of authors expressed herein do not necessarily state or reflect those of the United States government or Lawrence Livermore National Security, LLC, and shall not be used for advertising or product endorsement purposes.

Structure of the crust beneath Cameroon, West Africa, from the joint inversion of Rayleigh Wave Group Velocities and Receiver Functions.

Alain-Pierre K. Tokam[1], Charles T. Tabod[1], Andrew A. Nyblade[2], Jordi Julià[2], Douglas A. Wiens[3], Michael E. Pasyanos[4]

1. Department of Physics, University of Yaoundé 1, P. O. Box 812 Yaounde, Cameroon
2. Department of Geosciences, Pennsylvania State University, USA
3. Department of Earth and Planetary Sciences, University of Washington in St. Louis, USA
4. Earth Science Division, Lawrence Livermore National Laboratory, Livermore, California, USA

Abstract

Key words: Joint inversion, surface wave dispersion, Receiver functions, crustal structure, Congo craton, Panafrican mobile belt.

1. Introduction

The Cameroon Volcanic Line (CVL) is a major geologic feature that cuts across Cameroon from the south west to the north east. It is a unique volcanic lineament which has both an oceanic and a continental sector and consists of a chain of Tertiary to Recent, generally alkaline volcanoes stretching from the Atlantic island of Pagalu to the interior of the African continent (Figure.1). The oceanic sector includes the islands of Bioko (formerly Fernando Po) and São Tomé and Príncipe while the continental sector includes the Etinde, Cameroon, Manengouba, Bamboutos, Oku and Mandara mountains, as well as the Adamawa and Biu Plateaus.

In addition to the CVL, three other major tectonic features characterize the region: the Benue Trough located northwest of the CVL, the Central African Shear Zone (CASZ), trending N70°E, roughly parallel to the CVL, and the Congo Craton in southern Cameroon (Figure 1). The origin of the CVL is still the subject of considerable debate, with both plume and non-plume models invoked by many authors (e.g., Deruelle et al., 2007; Ngako et al, 2006; Ritsema and Allen, 2003; Burke, 2001; Ebinger and Sleep, 1998; Lee et al, 1994; Dorbath et al., 1986; Fairhead and Binks, 1991; King and Ritsema, 2000; Reusch et al., 2010).

Crustal structure beneath Cameroon has been investigated previously using active (Stuart et al, 1985) and passive (Dorbath et al., 1986; Tabod, 1991; Tabod et al, 1992; Plomerova et al, 1993) source seismic data, revealing a crust about 33 km thick at the south-western end of the continental portion of the CVL (Tabod, 1991) and the Adamawa Plateau, and thinner crust (23 km thick) beneath the Garoua Rift in the north (Stuart et al, 1985) (Figure 1). Estimates of crustal thickness obtained using gravity data show similar variations between the Garoua rift, Adamawa Plateau, and southern part of the CVL (Poudjom et al., 1995; Nnange et al., 2000).

In this study, we investigate further crustal structure beneath the CVL and the adjacent regions in Cameroon using 1-D shear wave velocity models obtained from the joint inversion of Rayleigh wave group velocities and P-receiver functions for 32 broadband seismic stations (Figure 2). From the 1-D shear wave velocity models, we obtain new insights into the composition and structure of the crust and upper mantle across Cameroon. After briefly reviewing the geological framework of Cameroon, we describe the data and the joint inversion method, and then interpret variations in crustal structure found beneath Cameroon in terms of the tectonic history of the region.

2. Tectonic setting

2.1. The Cameroon volcanic Line

The continental sector of the CVL can be divided into a southern part, which extends from the coast to the southern edge of the Adamawa Plateau, and a northern part, which consists of the Adamawa Plateau. Both parts of the CVL are underlain by PanAfrican basement rocks consisting mainly of schists and gneisses intruded by granites and diorites. Cretaceous sediments, mostly sandstones and small amounts of limestone and shales, are found in the coastal plain.

Volcanic rocks that comprise the CVL range in composition from basalts to trachytes. For example, Mt. Manengouba consists of basalt, trachyte and rhyolite lavas, Mt. Cameroon, the largest of the continental volcanoes, consists mainly of alkaline basalts (Hedberg, 1968), and Mt. Etinde, one of the older volcanoes, is made of nephelinitic lavas (Nkoumbou et al, 1995; Hedberg, 1968). Other examples include Mt. Bamboutos, which is made of alkali basalts and trachytes, and Mt. Oku, which consists of transitional basalt, quartz trachyte and rhyolite flows (Fitton and Dunlop, 1985). The Mandara Mountains, along the northern Cameroon-Nigeria

border where some of the oldest volcanic rocks are found (c. 34. Ma), consist of trachyte and rhyolite plugs and alkali basalt flows (Fitton and Dunlop, 1985).

Along the CVL, mantle-derived (ultramafic) xenoliths have been found in several locations in basaltic lavas (Figure 1; Deruelle et al., 1991, 2007; Princivalle et al., 2000). The xenoliths provide evidence for metasomatism within the upper mantle beneath the CVL (Deruelle et al., 2007).

2.2. The Benue Trough

The Benue trough is a NE-SW trending basin that extends from the Niger delta basin (Gulf of Guinea) to Lake Chad. Its origin is linked to the opening of the South Atlantic Ocean in the Cretaceous (Guiraud et Maurin, 1992). The Yola-Garoua or Garoua rift and Mamfe basin are eastward extensions of the trough into Cameroon. The similar Y-shape of the Benue trough and CVL (Fitton, 1987), together with the similarity in the composition of the alkali basalt in both the Benue trough and CVL (Coulon et al., 1996), suggest common geodynamic controls on their formation. For example, Guiraud and Maurin (1992) have argued that the orientation of the trough and CVL may be controlled by northeast-trending PanAfrican dextral shear zones.

2.3. The Oubanguides Belt and the Central African Shear Zone

Most of the Precambrian basement in Cameroon north of the Congo Craton belongs to the PanAfrican Oubanguides or North Equatorial fold belt (Poidevin, 1983; Nzenti et al., 1988). The Oubanguides Belt is a branch of the much larger Neoprotoerozoic PanAfrican – Brazilian Belt, which resulted from the collision between the São Francisco Craton, the Congo Craton, and the West African Craton during the formation of Gondwana (Castaing et al., 1994; Toteu et al., 2004). The Oubanguides Belt includes several mylonitic shear zones among which, most notably the Sanaga Fault and the Central African Shear Zone (CASZ) (Toteu et al., 2004) (Figure 1).

The CASZ is a major tectonic feature extending from the Darfur region in Sudan across central Africa to the Adamawa Plateau (Dorbath et al., 1986). From the Adamawa Plateau, the CASZ continues to the southwest, where it is known as the Foumban Shear Zone, before disappearing beneath the Tertiary to recent volcanic cover in southwestern Cameroon. The shear zone can also be traced into Brazil, where it is called the Pernambuco lineament (Burke et al., 1971; Browne and Fairhead, 1983).

2.4. The Congo Craton

The Congo Craton occupies a large part of Central Africa and its northern edge in southern Cameroon is referred to as the Ntem Complex (Vicat et al., 1996). The Ntem Complex consists predominantly of Archean rocks with some reworking in the Paleoproterozoic (Tchameni et al., 2001). The Archaean rocks are preserved in greenstone belts surrounded by tonalite-trondhjemite-granodiorite (TTG) suites (Tchameni et al., 2000; Nsifa, 2006; Tchameni et al, 2001). The Paleoproterozoic reworking of the Ntem Complex was contemporaneous with the Eburnean orogenic cycle. It is characterized by the intrusion of mafic doleritic dykes and ended with a thermal or hydrothermal event c. 1800 Ma (Nsifa, 2006; Tchameni et al., 2001).

The boundary between the Oubanguides belt and the Congo Craton in southern Cameroon is poorly known and extends to the northeast towards the Central African Republic (Boukeke, 1994; Toteu et al., 2004). Along this boundary, PanAfrican rocks overthrust the Ntem Complex, forming an intracrustal discontinuity (Boukeke, 1994).

3. Data and methodology

The data used for this study were recorded between January 2005 and February 2007 by the Cameroon Broadband Seismic Experiment, which consisted of 32 portable broadband

seismometers installed across the country (Figure 2). Each station was equipped with a broadband seismometer (Guralp 3T or Streckheisen STS-2), a 24-bit Reftek digitizer and a GPS clock. Data were recorded continuously at 40 samples per second. Eight stations were installed in January 2005 and operated for two years; the remaining 24 stations were operated only for the second year of the experiment. The station spacing was about 50 to 150 km.

Data from the Cameroon Broadband Seismic Experiment have been used to perform a joint inversion of P-wave receiver functions and Rayleigh wave group velocities. Receiver functions are time series that represent the radial impulse response of the shallow structure of the Earth in the vicinity of the seismic station (Langston, 1979). They can be used to image velocity contrasts across discontinuities, and when modeled jointly with Rayleigh wave group velocities, the non-uniqueness inherent in receiver function inversion can be reduced. (Julià et al., 2000).

3.1. Rayleigh wave group velocities

Fundamental mode Rayleigh-wave group velocities have been measured on 101 events of magnitude 5 and above with epicentral distances of less than 40° and recorded by the stations in Cameroon. A single station method was used for measuring the group velocities based on the multiple filter method of Dziewonski et al., (1969). Prior to making the measurements, the quality of each seismogram was checked and the instrument effect was removed.

The group velocity measurements were added to the database of similar measurements for Africa from Pasyanos (2005), and a tomographic inversion based on ray approximation was performed that increased the resolution of group velocity estimates within Cameroon compared to the group velocity maps published by Pasyanos (2005) and Pasyanos and Nyblade (2007). Figure 3 shows examples of the ray coverage and variations in group velocities for periods of 20, 40 and 60 seconds. Resolution tests of group velocity model indicate that the spatial resolution at periods most sensitive to crustal structure (~10-50 seconds) is 2 to 3 degrees, and thus the group

velocity models have sufficient resolution to image differences in group velocities between regions that are ~200 to 300 km wide. A single dispersion curve for each station from 7 to 100 seconds was obtained from the group velocity maps. The curves were smoothed using a 3-point running average before using them in the joint inversion.

3.2. Receiver Functions

Receiver Functions were computed using data from 69 teleseismic events that occurred at epicentral distances between 30° and 95° and that had magnitudes ≥5.5. Two overlapping frequency bands corresponding to Gaussian widths of a = 1.0 and a = 2.5 (corner frequencies of 0.5 Hz and 1.2 Hz respectively) were used to compute the receiver functions because they contain complementary information on the receiver structure under the station (Julià, 2007).

To compute the receiver functions, the selected waveforms were decimated to 10 samples per second, windowed between 10 s before and 100 s after the leading P arrival, de-trended, tapered, and high-pass filtered above 50 s to remove low-frequency, instrumental noise. Radial and transverse receiver functions were then obtained from the filtered traces by rotating the original horizontal components around the corresponding vertical component into the great-circle path, and applying the iterative, time domain deconvolution procedure of Ligorría and Ammon (1999) to the rotated traces, with 200 iterations.

The percentage of recovery of the original radial waveform was evaluated from the RMS misfit between the original radial waveform and the convolution of the radial receiver function with the original vertical component, and the events that were recovered to less than 85% were rejected. The remaining waveforms were visually inspected for coherence and similarity, and were then stacked and clustered by ray parameter and back azimuth. At least 3 waveforms were required to perform the stacks with the exception of station CM27, for which only two waveforms were successfully recovered.

The transverse receiver functions (not shown here, see Tokam, 2010) were computed to check the degree of lateral heterogeneity and isotropy of the propagating medium (Cassidy, 1992). Small amplitudes on the transverse component indicate a laterally homogeneous and isotropic media beneath a station. In general, compared to radial receiver functions, the transverse waveforms have small amplitudes, apart from the waveforms for stations CM09 and CM15, indicating for both of these stations a high degree of crustal heterogeneity.

3.3. Joint inversion

The joint inversion was performed using the method developed by Julià et al. (2000, 2003). The method is based on a linearized inversion procedure that minimizes a weighted combination of least squares norms for each data set, a model roughness norm, and a vector-difference norm between inverted and preset model parameters. The velocity models obtained are consequently a compromise between fitting the observations, model simplicity and a priori constraints. To make the contribution of each data set to the joint least squares misfit comparable, a normalization of the data set is necessary, and this is done using the number of data points and variance for each of the data sets. An influence factor is used to control the trade-off between fitting the receiver functions and the group velocity curves.

The starting model for the joint inversion assumes an isotropic medium with a 37.5 km thick crust and a linear shear wave velocity increase in the crust from 3.4 to 4.0 km/s overlying a flattened PREM model (Dziewonski and Anderson, 1981) for the mantle. Poisson's ratio was set to 0.25 for the crust and crustal densities were deduced from P-wave velocities through the empirical relationship of Berteussen (1977). The starting model consisted of constant velocity layers that increase in thickness with depth. The thickness of the first and second layers are respectively 1 and 2 km while the thickness increases to 2.5 km between 3 and 60.5 km depth, 5 km between 60.5 and 260.5 km depth, and 10 km below a depth of 260.5 km.

The models obtained from the inversion show a good fit to the group velocity curves and receiver functions with the exception of stations CM09, CM15 and CM27. In general, the group velocities below 10 s period are sensitive to shallow crustal structures and sedimentary basins. For periods up to 40 - 50 s, they are sensitive to the whole crust and between periods of 50 - 100s, they preferentially sample the uppermost mantle (Pasyanos, 2005). Consequently, models were constrained to PREM velocities (Dziewonski and Anderson, 1981) below 200 km depth in the inversion. A Poisson's ratio of 0.25 was assumed for the crust while the Poisson's ratio for the PREM model was used for the mantle.

3.4. Model uncertainties

The approach of Julià et al. (2008) was applied to check for laterally varying structures around each station. In this approach, receiver functions are stacked in groups by backazimuth and ray-parameter, and because the receiver functions were computed for each event at overlapping frequencies (a= 1.0 and a= 2.5), two receiver function stacks were obtained for each group. Each receiver function group was then jointly inverted with the corresponding group velocity curve to obtain a shear velocity model for that specific group. For comparison to the velocity models obtained for each group, an average S-velocity model was obtained by inverting all the receiver function in each group with the same dispersion curve. The procedure was applied to stations that have at least four groups of receiver functions. The result for station CM07 is illustrated in Figure 4.

In general, there should not be any significant variations between the models for the average and single groups for stratified, isotropic media (Kennett, 2002). Variations between the models should result from the interaction of the P-waves with lateral heterogeneities in the crust and upper mantle. For all of the stations, there is good agreement between models, as shown for station CM07 in Figure 4.

To estimate the uncertainties in the S-velocity models, we compute the standard deviation for the models obtained for each group of receiver function stacks. Estimates of uncertainties in shear velocity for stations with four or more groups are less than 0.2 km/s for crustal layers, and therefore we place the overall uncertainty in shear velocity 0.2 km/s for any given crustal layer in the model. This implies an uncertainty of 2 to 3 km in Moho depth for most stations where a rapid increase of velocity can be observed at the crust mantle-boundary, and no more than 5 km where a smoothly varying shear velocity is found indicating a gradational Moho.

4. Results

Data from two stations (CM08 and CM14) in the Cameroon network were not included in this study because not enough high quality waveforms were available for computing receiver functions. Results from the joint inversion for the remaining stations are shown on Figures 5 and 6 and summarized in Table 1.

Figure 5 shows the modeling results for each station, and in Figure 6 the shear wave velocity models are shown clustered by tectonic terrain. Crustal thickness beneath each station was determined by placing the Moho at the depth where the shear wave velocity exceeds 4.3 km/s. Shear wave velocities for typical lower crustal lithologies obtained by using experimentally determined P-wave velocities and Vp/Vs ratios (e.g., Christensen and Mooney, 1995; Christensen, 1996) show that shear wave velocities in the lower crust cannot be higher than 4.3 km/s. Therefore, we take shear wave velocities above 4.3 km/s to indicate the presence of lithologies with mantle compositions, and we place the Moho where the shear wave velocities exceed that value. For many stations, there is a significant increase in velocity at the depth at which the shear wave velocity exceeds 4.3 km/s, but for other stations the change in shear wave

velocity is gradational from the lowermost crust into the upper mantle.

4.1. CVL

As described in section 2.1, we split the CVL into a southern part, comprising the region to the southwest of the Adamawa Plateau, and a northern part, which is comprised of the Adamawa Plateau. Beneath the highland regions of the southern CVL, crustal thickness estimates are on average of about 36 km, compared to 28 and 31 km in the Kumba graben and Mamfe basin, respectively (Table 1). Beneath Mt. Cameroon (station CM09), the shear wave velocity is complicated, and at two depths the shear wave velocity reaches 4.3 km/s, making it difficult to determine crustal thickness (Figure 6).

An average crustal shear wave velocity of 3.7 km/s is found at most of the stations in the southern part of the CVL, and slightly slower (3.6 km/s) for the Mamfe basin and Kumba graben (Table 1). The models in Figures 5 and 6 show within the top 15 km of the upper crust the presence of a fast layer, with velocities of 3.6 - 3.8 km/s, creating the appearance of a low velocity zone in the mid-crust. The crust below 20 km depth for the southern part of the CVL has an average shear wave velocity of about 3.9 km/s and a thin higher velocity layer (Vs ≥ 4.0 km/s) at the base of the crust. The thickness of this high velocity layer is 2.5 km at most stations, but is thicker than that at a few stations (CM19, CM23 and CM27). The average uppermost mantle velocity, determined by computing the average velocity between the Moho and 60 km depth, is 4.4 - 4.5 km/s (Table 1).

The structure of the northern part of the CVL, on average, is very similar to the southern part. The Moho is on average at a depth of 36 km beneath the Adamawa uplift, the average crustal Vs is 3.7 km/s, the crust below 20 km depth has an average Vs of 3.9 km/s, and the high velocity layer at the base of the crust is either very thin or else absent (Figure 6 and Table 1).

4.2. Oubanguides Belt

Stations CM03, CM10, CM12, and CM17 are located in the part of the Oubanguides Belt not affected by the CVL. The crustal thickness varies from 36 to 43 km with an average crustal shear wave velocity of about 3.8 km/s for the area (Figure 6 and Table 1). For crust below 20 km depth, the shear velocity is 3.9 - 4.0 km/s, on average, and a high velocity layer is also observed at the base of the crust with a thickness of 5 – 8 km. The uppermost mantle has a shear wave velocity of 4.5 km/s, similar to the uppermost mantle velocity beneath the CVL.

4.3. Congo Craton

The Congo craton is characterized by a crustal thickness of 43 – 48 km with an average crustal shear wave velocity of 3.9 km/s. A fast layer (3.6-3.8 km/s) in the upper crust is visible in the velocity models for all the stations (Figure 6), and below this fast layer there is a gradual increase of velocity with depth to the Moho. The shear wave velocity below 20 km depth is 4.0 - 4.2 km/s, which is substantially faster compared to shear wave velocities in that depth range beneath the CVL and PanAfrican terrain. This high velocity layer is the prominent feature of the lower crust across northern part of the Congo Craton. The Congo Craton crust is underlain by uppermost mantle with an average shear wave velocity of 4.6 km/s.

4.4. Coastal plain

The Moho at stations CM01 and CM05 is found at a depth of 28 km (Table 1). The fast layer in the upper crust can be seen in velocity models for both stations, as well as an average lower crustal shear wave velocity of 4.1 km/s. The terrain is underlain by uppermost mantle with a shear wave velocity of 4.4 km/s.

4.5. Garoua Rift

The crustal thickness is variable across this part of Cameroon. The Moho is found at depth of 26 km beneath station CM29, and 31 to 33 km beneath stations CM28, CM31 and

CM31 to the north and south of the rift. The average crustal shear wave velocity is about 3.4 – 3.5 km/s across the region. The upper crustal structure is characterized by a shallow, thin layer with a low shear wave velocity (Vs < 3km/s). The shear wave velocity below 20 km is variable with an average of 3.7 – 3.9 km/s for the region. The average uppermost mantle shear wave velocity is 4.3 – 4.4 km/s across the region, which is somewhat slower compared to the uppermost mantle velocity for the other parts of Cameroon.

5. Discussion

To summarize, there are four main findings that come from the joint inversion of the receiver functions and Rayleigh wave group velocity curves. 1) Crustal structure is similar beneath the CVL, including the Adamawa Plateau, and the Oubanguides Belt to the south of the CVL. 2) The crust is thicker under the Congo Craton than the Oubanguides Belt and is characterized by shear wave velocities ≥ 4.0 km/s in the lower part of the crust. 3) Thinner crust is found under the Garoura rift and the coastal plain. 4) A fast velocity layer (Vs of 3.6 to 3.8 km/s) in the upper crust is found beneath many of the seismic stations, and is not confined to just one region. In this section, first briefly compare our results to previously published results on crustal structure in Cameroon and then examine to what extent, if any, these findings, as well as the average structure of the crust of each region, are anomalous with respect the structure of similar aged crust in other parts of Africa.

5.1 Comparison with previous estimates of crustal structure

Our estimates of crustal thickness are in good agreement with previous estimates based on both gravity and seismic data for a number of regions (Table 2). Many of these estimates come from interpreting gravity data, and in Figure 7 we show that there is a strong correlation between

crustal thickness and Bouguer gravity anomalies along the length of the CVL. Small departures between the Bouguer gravity anomaly and crustal thickness can be attributed to near-surface structure. For example, the small decrease in the Bouguer anomaly around station CM29 is likely the effect of 3-4 km of sediments in the Garoura rift (Stuart et al., 1985), while the small increase at station CM25 correlates with the high velocity layer in the upper crust beneath this station.

The correlation between the Bouguer gravity anomaly and crustal thickness also corroborates our choice of crustal thickness on the velocity profile for station CM09. On that profile, there are two depths at which the shear wave velocity increases to > 4.3 km/s, one at 25.5 km and the other at 40.5 km. Our placement of the Moho at the shallower discontinuity is consistent with the Bouguer gravity anomaly, which indicates a thin crust beneath CM09 (Figure 7).

5.2 Comparison with crustal structure in other parts of Africa

For the comparison of crustal structure in Cameroon to elsewhere in Africa, we use the structure of crust in eastern and southern Africa, where the structure of Archean and Proterozoic crust has been well imaged using the same methods as used in this study for Cameroon. The relevant details of crustal structure are summarized in Table 3.

5.2.1 PanAfrican - The Mozambique Belt in eastern Africa developed during the PanAfrican orogenic event along the eastern side of the Archean Tanzania Craton. The structure of the Mozambique Belt crust has been well studied using the joint inversion of receiver functions and Rayleigh wave group and phase velocities (Julia et al. 2005; Dugda et al., 2009), and also by seismic refraction profiling (Fuchs et al., 1997 and references therein).

The crustal thickness beneath the Mozambique Belt varies between 36 and 42 km with an average of 38 km. The bottom of the Mozambique Belt is characterized by a 5 to 10 km thick

layer of high velocity (Vs ≥ 3.9 km/s) rock, indicating a mafic lithology. Crustal structure beneath the PanAfrican Oubanguides Belt, including the southern CVL and Adamawa Plateau, is very similar to the Mozambique Belt, with crustal thickness ranging between 36 and 43 km and a high velocity layer at the base of the crust with a thickness of 5 to 8 km. Therefore, the CVL appears to have not affected the bulk crustal structure of the PanAfrican crust in Cameroon. Certainly the crust under some of the stations along the CVL has been perturbed by the magmatism, but overall there is no discernable modification to average crustal structure, at least not within the resolution of the joint inversion method used in this study.

In contrast to that conclusion, the PanAfrican crust under the Garoura rift and coastal plain has been thinned by 10 or more kilometers. However, this thinning has not resulted from the CVL but rather from other tectonic events. The crust beneath the coastal plain was probably thinned during the opening of the southern Atlantic Ocean, while the crust beneath the Garoura rift was thinned during the formation of the Benue Trough in the early Cretaceous (Kamguia et al., 2005; Stuart et al., 1985; Baudin, 1991).

5.2.2. Congo Craton - Using the joint inversion of receiver functions and Rayleigh wave group and phase velocities, crustal structure of the Tanzanian Craton has been imaged by Julia et al. (2005) and crustal structure of the Zimbabwe and Kaapvaal Cratons has been imaged by Kgaswane et al. (2009). The Tanzania Craton is underlain by crust that is between 38 and 42 km thick with and average of 40 km, while crustal thickness beneath Kaapvaal and Zimbabwe cratons is between 36 and 40 km, with averages of 38 and 36 kms, respectively. The average thickness of the high velocity (mafic) lower crust is 10 km or less for all three cratons.

In comparison, the crust beneath the Congo Craton, which ranges from 43 to 48 kms, is significantly thicker, and the high velocity layer in the lowermost crust is also much thicker. The average thickness of the high velocity layer is 23 km, more than 10 km thicker than that found

beneath the other cratons (Table 3). Interestingly, the thickness of the high velocity layer is as thick as or thicker than the high velocity layer found beneath the Bushveld Complex in the northern part of the Kaapvaal Craton or the Limpopo Belt, which represents the Archean suture between the Zimbabwe and Kaapvaal cratons (Kgaswane et al., 2009).

Examining magmatic events that post-date the formation of the Ntem Complex do not provide much help in explaining the very thick mafic lower crust. Mafic dikes older than 2100 Ma associated with the rifting of the Ntem Complex crust, as well as the intrusion of gabbros and the development of greenstone belts, provide evidence for magmatic events that could have added mafic rock to the lower crust (Nsifa, 2006; Vicat et al., 1996; Maurizot et al., 1986; Tchameni et al., 2000; Shang et al., 2004; Tchameni et al. 2001), but similar tectono-magmatic events have affected the Tanzania, Zimbabwe and Kaapvaal cratons and therefore are not unique to the Ntem Complex. In addition, there is no indication that a magmatic event equivalent in scale to the Bushveld has affected the Ntem Complex, and so such an event can also be ruled out as a possible explanation for the thick mafic lower crustal layer of the Ntem Complex.

The remaining possibility is that the northern boundary of the Congo Craton is a large suture zone that formed during the PanAfrican orogeny, and that both the thickened crust and the thick mafic lower crustal layer are relict features from a continent-continent collision during the formation of Gondwana. A suture zone between the Congo Craton and the Oubanguides Belt has been suggested in several studies (e.g. Penaye et al., 1993; Tadjou et al., 2009; Toteu et al., 2004), although the exact location of the suture is still a matter of some debate.

In Precambrian sutures elsewhere (e.g., the Limpopo (Kgaswane et al., 2009; the Superior Province (Gibb et al., 1983), the Tanzania Craton (Nyblade and Pollack, 1992), the Yilgarn Craton (Mathur, 1974; Wellmann,1978), the Indian shield (Subrahmanyam, 1978), the Mann shield (Blot et al., 1962; Louis, 1978; Black et al., 1979)), 5–10 km of crustal thickening is

observed along with the presence of mafic units in a crust commonly affected by granulite facies metamorphism and extraction of a felsic partial melt component. Both the thicker crust and the large thickness of lower crust with high shear wave velocities of the Ntem Complex is consistent with typical ‘‘suture’’ thickened crust found in other Precambrian terrains, and thus we suggest this as a plausible explanation for the anomalous crustal structure beneath the Ntem Complex.

5.3. Fast upper crustal layer

At many stations within all of the regions in Cameroon, a fast (Vs of 3.6 to 3.8 km/s) layer in the upper crust can be seen (Figure 6), indicating a fair amount of heterogeneity within the upper crust both within and between regions. We interpret these layers generically as mafic bodies intruded into the upper crust during magmatic events of various ages. The occurrence of ultramafic xenoliths along the CVL (Nkombou et al., 1997; Deruelle et al., 2007) supports this interpretation, at least for the regions of Cenozoic volcanism. A detailed treatment of the origin of the intrusions is beyond the scope of this study and is focus of ongoing research.

6. Summary and Conclusions

A joint inversion of Rayleigh wave group velocities and receiver functions has been used to investigate the structure of the crust beneath Cameroon. The main findings are that 1) crustal structure is similar beneath the CVL, which includes the Adamawa Plateau, and the Oubanguides Belt to the south of the CVL, 2) the crust is thicker under the Congo Craton than the Oubanguides Belt and is characterized by shear wave velocities $\geq$ 4.0 km/s in the lower part of the crust, 3) thinner crust is found under the Garoura rift and the coastal plain., and 4) a fast velocity layer (Vs of 3.6 to 3.8 km/s) in the upper crust is found beneath many of the seismic

stations, and is not confined to just one region. Our estimates of crustal thickness are in good agreement with previous estimates based on both gravity and seismic data for a number of areas within Cameroon.

We have compared crustal structure in Cameroon to the structure of crust in eastern and southern Africa, where the structure of Archean and Proterozoic crust has been well imaged using the same methods as in this study. Crustal structure beneath the PanAfrican Oubanguides Belt, including the southern CVL and Adamawa Plateau, is very similar to the Mozambique Belt, and therefore the CVL appears to have not affected the bulk crustal structure of the PanAfrican crust in Cameroon. However, the PanAfrican crust under the Garoura rift and coastal plain has been thinned by 10 or more kilometers. The crust beneath the coastal plain was probably thinned during the opening of the southern Atlantic Ocean, while the crust beneath the Garoura rift was thinned during the formation of the Benue Trough in the early Cretaceous.

In comparison, the crust beneath the Congo Craton is significantly thicker than beneath other parts of Cameroon and is, on average, also significantly thicker than the crust beneath the Tanzania, Kaapvaal and Zimbabwe cratons. In addition, the Congo Craton crust has a high velocity layer in the lowermost crust is more than 10 km thicker than that found beneath the other cratons. We suggest that northern boundary of the Congo Craton could be a large suture zone that formed during the PanAfrican orogeny, and that both the thickened crust and the thick mafic lower crustal layer are relict features from a continent-continent collision during the formation of Gondwana.

This work performed under the auspices of the U.S. DOE by LLNL under Contract DE-AC52-07NA27344.

Acknowledgements

Penn State University and Washington University in St Louis supported APKT in the USA where part of this work was carried out. The Abdu Salam Centre for Theoretical Physics (ICTP) supported CTT through the Associate Scheme. Most of figures were prepared using the GMT software. We would like to thank Charles Ammon, Yongcheol Park, Mulugeta Dugda and Eldridge Kgaswane for assistance with computer codes.

References

Baudin, P., 1991. *Le magmatisme mésozoïque a cénozoïque du fossé de la Bénoué (Nigeria). Géochronologie, pétrogenèse, cadre géodynamique*. Ph.D Thesis, Université Aix-Marseille III, France.

Berteussen, K.A., 1977. Moho depth determinations based on spectral ratio analysis of NORSAR long-period P waves. *Phys. Earth Planet. Inter*., **15**, 13–27.

Black, R., Caby, R., Moussine-Pouchkine, A., Bertad, J.M, Boullier A.M., Fabre, J. & Lesquer, A., 1979. Evidence for late Precambrian plate tectonics in West Africa. *Nature*, **278**, 223 – 227.

Blot, C., Crenn, Y. & Rechenmann, R., 1962. Elements apportes par la gravimetrie a la connaissance de la tectonique profonde du Senegal. *C.R. Acad. Sci. Paris*, **254**, 1131 – 1133.

Boukeke D. B., 1994. *Structures crustales d'Afrique Centrale déduites des anomalies gravimétriques et magnétiques: le domaine précambrien de la République Centrafricaine et du Sud Cameroun*. PhD Thesis, Univ. Paris XI, Orsay.

Browne, J. D. & Fairhead, J. D., 1983. Gravity study of the Central African Rift System: a model of continental disruption, 1, The Ngaoundere and Abu Gabra Rifts. *Tectonophysics*, **94**, 187-203.

Burke K., Dessauvagie, T.F.J. & Whiteman, A.J., 1971. The opening of the Gulf of Guinea and the geological history of the Benue Trough and Niger delta. *Nature Phys. Sci.,* **233**, 51-55

Burke, K., 2001. Origin of the Cameroon line of volcano-capped swells. *Journal of Geology*, **109(3)**, 349–362.

Cassidy, J., 1992. Numerical experiments in broadband receiver function analysis. *Bull. Seismol. Soc. Am.*, **82**, 1453– 1474.

Castaing, C., Feybesse, J.L., Thieblemont, D., Triboulet, C. & Chevremont, P., 1994. Palaeogeographical reconstructions of the Pan-African/Brasiliano orogen: closure of an oceanic domain or intracontinental convergence between major blocks?. *Precambrian Research*, **67**, 327–344.

Christensen, N. I. & Mooney, W.D., 1995. Seismic velocity structure and composition of the continental crust: A global view. *J. Geophys. Res.*, **100(B7)**, 9761-9788.

Christensen N. I., 1996. Poisson's ratio and crustal seismology. *J. Geophys. Res.*, **101**, 3139–3156.

Coulon, C., Vidal, P., Dupuy, C., Baudin, P., Popoff, M., Maluski, H. & Hermitte, D., 1996. The Mesozoic to early Cenozoic magmatism of the Benue Trough (Nigeria); geochemical evidence for the involvement of the St. Helena plume. *Journal of Petrology,* **37**, 1341–1358.

Déruelle B., Ngounouno, I., & Demaiffe, D., 2007. The Cameroon Hot Line (CHL): A unique example of active alkaline intraplate structure in both oceanic and continental lithospheres. *C. R. Geoscience*, **339**, 589–600.

Déruelle B., Nkombou, C., Kambou, R., Lissom, J., Njongfang, E., Ghogomu, R.T. & Nono, A., 1991. The Cameroon Line: a review, in *: A.B. Kampunzu, R.T. Lubala (Eds.), Magmatism in Extensional Structural Settings. The Phanerozoic African Plate . Springer-Verlag*, **79**, 25–45. 9

Dorbath C., Fairhead, J.D. & Stuart, G.W., 1986. A teleseismic delay time study across the Central African Shear Zone in the Adamawa region of Cameroon. *Geophys. J. R. Astr. Soc*., **86**, 751–766.

Dugda M. T., Nyblade, A. A., & Julia, J., 2009. S-wave velocity structure of the crust and upper mantle beneath Kenya in comparison to Tanzania and Ethiopia: Implications for the formation of the East African and Ethiopian Plateaus. *South African Journal of Geology*, 112, 241-250.

Dziewonski A., Bloch, S. & N. Landisman, 1969. A technique for the analysis of transient seismic signals. *Bull. Seism. Soc. Am*., **59**, 427-444.

Dziewonski A.M. & Anderson, D.L., 1981. Preliminary reference earth model. *Phys. Earth planet. Int*., **25**, 297–356.

Ebinger C.J. & Sleep, N.H., 1998. Cenozoic magmatism throughout east Africa resulting from impact of a single plume. *Nature*, **395**, 788–791.

Fairhead, J.D. & Okereke, C.S., 1987. A regional gravity study of the West African rift system in Nigeria and Cameroon and its tectonic interpretation. *Tectonophysics*, **143**, 141-159.

Fairhead, J.D. & Binks R.M., 1991. Differential opening of the central and south-atlantic oceans and the opening of the West African Rift System. *Tectonophysics*, **187 (1-3),** 191-203.

Fitton, J.G., 1987. The Cameroon Line, West Africa: a comparison between oceanic and continental alkaline volcanism. Alkali igneous rocks. *Geol. Soc. Spec. Publ.*, **30**, 273-291.

Fitton, J.G. & Dunlop H.M., 1985. The Cameroon Line, West Africa, and its bearing on the origin of oceanic and continental alkali basalt. *Earth Planet. Sci. Lett*., **72**, 23–38.

Fuchs, K., Altherr, B., Muller,B. & Prodehl, C., 1997. Structure and dynamic processes in the lithosphere of the Afro-Arabian rift system, *Tectonophysics,* **278,** 1–352.

Gibb, R. A., Thomas, M.D., Lapointe, P. & Mukhopadhay, M., 1983. Geophysics of proposed Proterozoic sutures in Canada. *Precambrian Research,* **19**, 349 – 384.

Guiraud, R. and Maurin, C.J., 1992. Early Cretaceous rifts of Western and Central Africa. *Tectonophysics*, **213**, 153-168.

Hedberg, J.D., 1968. *A geological Analysis of the Cameroon Trend*. Ph. D. thesis, University of Princeton.

Julià, J., Ammon, C.J., Herrmann, R.B. & Correig, A.M., 2000. Joint inversion of receiver function and surface wave dispersion observations. *Geophys. J. Int.,* **143**, 99–112.

Julià, J., Ammon, C. J. & Herrmann, R.B., 2003. Lithospheric structure of the Arabian Shield from the joint inversion of receiver functions and surface wave group velocities. *Tectonophysics*, **371**, 1 –21.

Julià, J., Ammon, C.J. & Nyblade, A.A., 2005. Evidence for mafic lower crust in Tanzania, East Africa, from joint inversion of receiver functions and Rayleigh wave dispersion velocities. *Geophys. J. Int.*, 162, 555–562.

Julià J., 2007. Constraining velocity and density contrasts across the crust– mantle boundary with receiver function amplitudes. *Geophys. J. Int.*, **171**, 286– 301.

Julià, J., Assumpção, M. & Rocha, M.P., 2008. Deep crustal structure of the Paranã Basin from receiver functions and Rayleigh-wave dispersion: Evidence for a fragmented cratonic root. *Journal of Geophysical Research*, **113**, B08318, doi:10.1029/2007JB005374.

Kamguia J., Manguelle-Dicoum, E., Tabod, C.T. & Tadjou, J.M., 2005. Geological models deduced from gravity data in the Garoua basin, Cameroon. . *Journal of Geophys. Eng.*, **2**, 147-152.

Kamguia J., Nouayou, R., Tabod, C.T., Tadjou, J.M., Manguelle-Dicoum, E. and Kande, H.L., 2008. Geophysical signature of geological units inferred from the analysis of geoid maps in Cameroon and its surroundings. *Journal of African Earth Sciences*, **52**, 1-8.

Kennett B. L. N., 2002. *The seismic wavefield*. Vol II: Interpretation of seismograms on regional and global scales. Cambridge University Press.

Kgaswane, E.M, Nyblade, A.A., Julià, J., Dirks, P.H.G.M., Durrheim R.J. & Pasyanos, M.E., 2009. Shear Wave Velocity Structure of the Lower Crust in Southern Africa: Evidence for Compositional Heterogeneity within Archaean and Proterozoic Terrains. *J. Geophys. Res.*, **114**, B12304, doi:10.1029/2008JB006217.

King, S.D. & Ritsema, J., 2000. African hot spot volcanism: Small-scale convection in the upper mantle beneath cratons. *Science*, **290**, 1137–1140.

Langston, C.A., 1979. Structure under Mount Rainier,Washington, inferred from teleseismic body waves. *J. Geophys. Res.*, **84**, 4749–4762.

Lee, D.C., Halliday, A., Fitton, J.G. & Poli, G., 1994. Isotopic Variations With Distance And Time In The Volcanic Islands Of The Cameroon Line – Evidence For A Mantle Plume Origin. *Earth And Planetary Science Letters*, **123**(1- 4), 119–138.

Ligorría, J.P. & C.J. Ammon, 1999. Iterative deconvolution and receiver function estimation. *Bull. seism. Soc. Am.*, **89**, 1395–1400.

Louis P., 1978. Gravimetrie et geologie en Afrique occidentale et centrale. *Mem. Bur. Rech. Geol. Min.*, **91**, 53 – 61.

Mathur, S.P., 1974. Crustal structure in southwestern Australia from seismic and gravity data. *Tectonophysics*, **24**, 151 – 182.

Maurizot P., Abossolo, A., Feybesse, A., Johan, J.L. & P. Lecomte, 1986. Etude et prospection miniere du Sud-Ouest Cameroun. Synthese des travaux de 1978 a 1985. *Rapport B.R.G.M,* **85**, CMR 066, Janvier 1986, 274 P.

Nnange, J.M., Ngako, V., Fairhead, J.D. & Ebinger, C. J., 2000. Depths to density discontinuities beneath the Adamawa Plateau region, Central Africa, from spectral analysis of new and existing gravity data. *Journal of African Earth Sciences*, **30** (4), 887 – 901.

Ngako V., Njonfang, E, Tongwa, A.F., Affaton, P., & Nnange, J.M., 2006. The North-South Paleozoic to Quaternary trend of alkaline magmatism from Niger-Nigeria to Cameroon: Complex interaction between hotspots and Precambrian faults. *Journal of African Earth Sciences*, **45**, 241–256.

Nkoumbou C., Deruelle, B. & Velde, D., 1995. Petrology of Mt. Etinde nephelinite series. *Journal of Petrology*, **36**, 373–395.

Nsifa, N.E., 2006. *Magmatisme et Evolution géodynamique de l'Archéen au Protérozoïque de la bordure nord-ouest du Craton du Congo (Complexe du Ntem) au Sud-Ouest Cameroun*. Thèse de Doctorat d'Etat, Faculté des Sciences, Université de Yaounde 1.

Nyblade, A.A. & Pollack, H.N., 1992. A gravity model for the lithosphere in western Kenya and northeastern Tanzania. *Tectonophysics*, **212**, 257 – 267.

Nzenti, J.P., Barbey, P., Macaudière, J., & Soba, D., 1988. Origin and evolution of the late Precambrian high-grade Yaoundé gneisses (Cameroon). *Precambrian Research*, **38**, 91–109.

Pasyanos, M.E., 2005. A variable resolution surface wave dispersion study of Eurasia, North Africa, and surrounding regions. *J. of Geophys. Res.*, **110,** B12301, doi:10.1029/2005JB003749.

Pasyanos, M.E. & Nyblade, A.A., 2007. A Top to Bottom Lithospheric Study of Africa and Arabia. *Tectonophysics*, **444**(1-4), 27–44.

Penaye, J., Toteu, S.F., Michard, A., Van Schmus, W.R. & Nzenti, J. P., 1993. U-Pb and Sm-Nd preliminary geochronologic data on the Yaoundé serie, Cameroon: reinterpretation of granulitic rock as the suture of the collision in the « Centrafricain » belt. *Compte Rendu Académie des Sciences,* **317**, 789-794.

Plomerova, J., Babuska, V., Dorbath, L., Dorbath, R. & Lillie, R.J., 1993. Deep lithospheric structure across the Central African Shear Zone in Cameroon. *Geophys. J. Int.*, **115**, 381–390.

Poidevin, J.L. 1983. La tectonique pan-africaine à la bordure nord du craton congolais: l'orogenèse des Oubanguides, i*n 12th colloque on the African Geology*. Musée Royal de l'Afrique Centrale, Tervuren, Belgium. Abstract, p. 75.

Poudjom, D.Y.H., Nnange, J.M., Diament, M., Ebinger, C.J. & Fairhead, J.D., 1995. Effective elastic thickness and crustal thickness variation in West Central Africa inferred from gravity data. *Journal of Geophysical Research*, **100**(B11), 22,047–22,070.

Princivalle F., Salviulo, G., Marzoli, A. & Piccirillo, E.M., 2000. Clinopyroxene of spinel-peridotite mantle xenoliths from Lake Nji (Cameroon Volcanic Line, W Africa): crystal chemistry and petrological implications. *Contrib. Mineral. Petrol*., **139**, 503–508.

Reusch et al. 2010. ?????????? .

Ritsema, J. & Allen, R.M., 2003. The elusive mantle plume, Earth planet. *Sci. Lett*., **207**, 1–12.

Rudnick, R.L. & Gao, S., 2003. Composition of the Continental Crust, in *Treatise on Geochemistry*, pp. 1–64, Vol. 3, Elsevier.

Shang C.K., Satir, M., Siebel, W., Nsifa, E. N., Taubald, H., Liegeois, J. P. & Tchoua, F.M., 2004. TTG magmatism in the Congo craton; a view from major and trace element geochemistry, Rb-Sr and Sm-Nd systematics: case of the Sangmelima region, Ntem complex, southern Cameroon. *Journal of African Earth Sciences*, **40**, 61-79.

Stuart, G.W., Fairhead, J.D., Dorbath, L. and Dorbath, C., 1985. A seismic refraction study of the crustal structure associated with the Adamawa plateau and Garoua rift, Cameroon, West Africa. *Geophys. J. R. Astron. Soc*., **81**, 1-12.

Subrahmanyam, C.,1978. On the relation of gravity anomalies to geotectonics of the Precambrian terrains of the south Indian shield. *Journal of Geological Society of India*, **19**, 251 – 263.

Tabod, C.T., 1991. *Seismological studies of the Cameroon Volcanic Line, in West Africa*. Ph. D. thesis, University of Leeds.

Tabod, C.T., Fairhead, J.D., Stuart, G.W., Ateba, B. and Ntepe, N., 1992. Seismicity of the Cameroon Volcanic Line, 1982–1990. *Tectonophysics,* **212,** 303–320.

Tadjou J. M., Nouayou, R., Kamguia, J., Kande, H. L. & Manguelle-Dicoum, E., 2009. Gravity analysis of the boundary between the Congo craton and the Pan-African belt of Cameroon. *Austrian Journal of Earth Sciences*, **102**, 71-79.

Tchameni, R., Mezger, K., Nsifa, N.E. & Pouclet, A., 2000. Neoarchaean crustal evolution in the Congo Craton: evidence from K rich granitoids of the Ntem Complex, southern Cameroon. *Journal of African Earth Sciences*, **30** (1), 133-147.

Tchameni R., Mezger, K., Nsifa, N.E. & Pouclet, A., 2001. Crustal origin of Early Proterozoic syenites in the Congo Craton (Ntem Complex), south Cameroon. *Lithos*, **57**, 23-42.

Tokam, K. A. P., 2010. *Crustal structure beneath Cameroon (West Africa) deduced from the joint inversion of Rayleigh wave group velocities and receiver functions*. PhD thesis, University of Yaounde 1, Cameroon.

Toteu, S.F., Penaye, J., Poudjom Djomani, Y., 2004. Geodynamic evolution of the Pan-African Belt in Central Africa with special reference to Cameroon. *Can. J. of Earth Science*, **41**, 73-85. doi: 10.1139/E03-079

Vicat J.P., Leger, J.M., Nsifa, E., Piguet, P., Nzenti, J.P., Tchameni, R. and Pouclet, A., 1996. Distinction au sein du craton congolais du Sud-Ouest du Cameroun, de deux épisodes doléritiques initiant les cycles orogéniques éburnéen (Paléoprotérozoïque) et Pan-Africain (Néoprotérozoïque). *Compte Rendu de l'Académie des Sciences*, *série IIa* **,323**, 575-582.

Wellmann, P., 1978. Gravity evidence for abrupt changes in the mean crustal density at the junction of Australian crustal blocks. *Aust. Bur. Miner. Resour. Geol. Geophys. Bull.*, **3**, 153 – 162.

Table 1. Summary of crustal structure by geological terrains shown in figure 6.

Terrain		Stations	Crustal thickness (km)	Average crustal thickness ± standard deviation (km)	Average Uppermost mantle Vs (km/s)	Average crustal Vs (km/s)		Average Vs below 20 km depth (km)		Average thickness of layers with Vs ≥ 4.0 km/s (km)	
Coastal plain		CM01	28	28	4.4	3.6	3.7	4.1	4.1	10	10
		CM05	28			3.7		4.1		10	
Congo craton		CM02	43	44.7 ± 1.5	4.6	3.8	3.9	4.0	4.1	18	22.8
		CM04	45.5			3.9		4.1		25.5	
		CM06	45.5			3.9		4.2		27.5	
		CM07	43	45.5 ± 2.5	4.6	3.9	3.9	4.1	4.1	20	
		CM11	48			3.9		4.1		22.5	
Panafrican		CM03	43	38.6 ± 3.1	4.5	3.8	3.8	3.9	3.9	5	6.3
		CM10	38			3.8		4.0		7.5	
		CM12	38			3.8		3.9		7.5	
		CM17	35.5			3.7		3.9		5	
Southern CVL	Mt Cameroon	CM09	**25.5 ?**	-	-	-		-	-	-	-
	High lands	CM15	33	35.5 ± 3.1	4.5	3.6	3.7	3.9	3.9	2.5	5
		CM16	35.5			3.7		3.9		5	
		CM19	35.5			3.7		3.9		5	
		CM20	33			3.7		3.9		2.5	
		CM23	40.5			3.7		4.0		10	
	Kumba graben	CM13	28	29.2 ± 1.8	4.4	3.6	3.6	3.8	3.8	2.5	2.5
	Mamfe basin	CM18	30.5			3.6		3.9	3.9	2.5	2.5
Adamawa Plateau (northeastern CVL)		CM21	35.5	35.5 ± 1.6	4.4	3.7	3.7	3.9	3.9	2.5	2
		CM22	35.5			3.7		3.9		2.5	
		CM24	35.5			3.7		3.8		-	
		CM25	38			3.7		3.9		2.5	
		CM26	33			3.6		3.8		-	
		CM27	35.5			3.7		3.9		5.0	
Garoua Rift terrain	South of Garoua rift	CM28	30.5	30.5	4.3	3.5	3.5	3.8	3.8	2.5	2.5
	Garoua rift	CM29	25.5	25.5	4.3	3.4	3.4	3.7	3.7	-	-
	North of Garoua rift	CM30	28	30.5 ± 2.5	4.4	3.4	3.5	3.7	3.8	-	2
		CM31	30.5			3.5		3.9		2.5	
		CM32	33			3.5		3.9		2.5	

Table 2. Comparision of crustal thickness estimates from this study with crustal thickness estimates from previous studies

	Average crustal thickness (km)		**Type of data used**	**References**
	This study	Other studies		
Garoua Rift	25.5	23 24	Seismic Gravity	Stuart et al., 1985 Kamguia et al., 2005
CVL in general CVL southern part	- 35.5	30-34 ~ 33	Gravity Seismic	Fairhead and Okereke (1987) Tabod, 1991.
Adamawa Plateau	35.5	33 33	Seismic Gravity	Stuart et al., 1985 Nnange et al., 2000
Congo craton	45.0	50 ± 10	Gravity	Poudjom et al., 1995

Table 3. Comparison of crustal structure in Cameroon to similar aged terrains in eastern and southern Africa.

Eastern Africa			**Southern Africa**			**Cameroon**		
Terrain	**Average Moho depth (km)**	**Average mafic layer thickness (km)**	**Terrain**	**Average Moho depth (km)**	**Average Mafic layer thickness (km)**	**Terrain**	**Average Moho depth (km)**	**Average Mafic layer thickness (km)**
Tanzania craton	40 ± 3	< 10	Zimbabwe craton	36 ± 1	10 ± 4	Congo craton	45 ± 2	23 ± 4
			Kaapval craton	38 ± 3	9 ± 5			
			Bushveld Complex	41 ± 3	10			
Mozambique belt	38 ± 3	< 10	Limpopo belt	41 ± 3	14 ± 2	Oubanguides Belt	39 ± 3	6 ± 2
						CVL	36 ± 3	5 ± 3
						Garoua rift	26 ± 3	2 ± 1
Julià et al. (2005)			**Kgaswane et al. (2009)**			**This study**		

Figures.

Figure 1. Simplified geological map of the study area. Volcanic areas that are part of the CVL are shown in red. The approximate northern boundary of the Congo Craton is shown with a green dashed line, and the small solid circles show approximate location of xenolith ocurrances. FSZ- Foumban shear zone. CASZ - Central African shear zone.

Figure 2 : Color elevation map showing seismic station locations and shear zones. The dashed light blue line shows the location of the profile in Figure 1.

Figure 3: Rayleigh wave group velocity maps from an updated version of the maps presented in Pasyanos (2005). Top left - ray coverage for 20 sec Rayleigh waves. Other panels show group velocities for the periods indicated above each panel.

Figure 4: a) Joint inversion results for station CM07 for individual groups of receiver functions. The top, middle and bottom panels in each column display receiver functions, group velocities and shear wave velocity models, respectively. Observations are shown in black and predictions in red. b) Shear wave velocity models obtained using the whole group of receiver functions. c) Superposition of single (red) and full joint inversion models to assess the uncertainties.

Figure 5: Joint inversion results for all stations used in this study. Each column shows results for a single station. The top, middle and bottom panels in each column display receiver functions, group velocities and shear wave velocity models, respectively.

Figure 6: Shear wave velocity profiles grouped by tectonic terrain. Lines on each profile are shown for reference. The solid line is at 4.0 km/a and the dashed line at 4.3 km/s).

Figure 7 : Top - Crustal thickness along the profile shown in Figure 1. Bottom - point Bouguer anomalies along the same profile, extracted from the simple Bouguer gravity anomaly map of Kamguia et al. (2008).

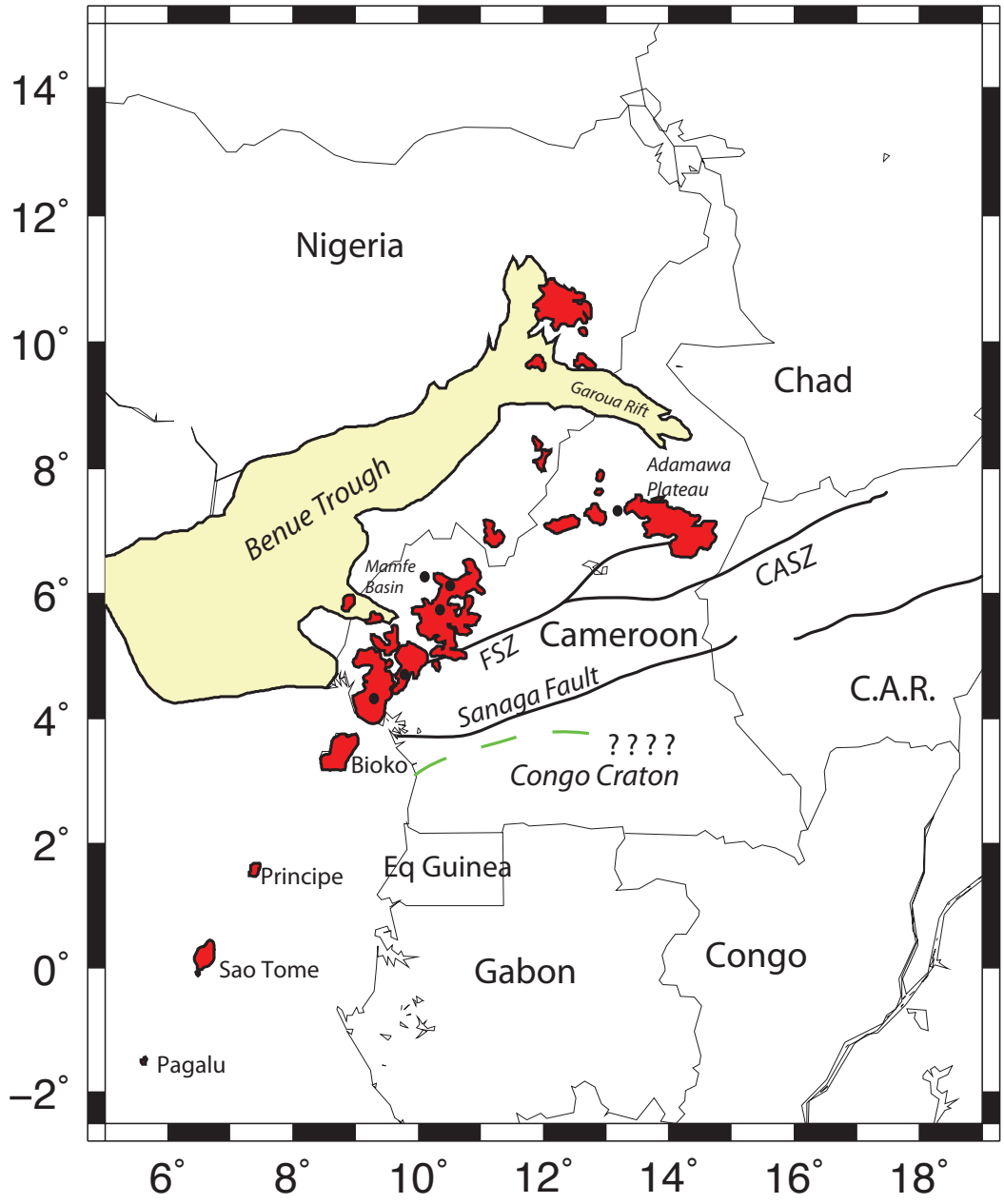
Nigeria
Chad
Garoua Rift
Adamawa Plateau
Benue Trough
Mamfe Basin
CASZ
FSZ
Cameroon
Sanaga Fault
C.A.R.
? ? ? ?
Congo Craton
Bioko
Principe
Eq Guinea
Sao Tome
Gabon
Congo
Pagalu
14°
12°
10°
8°
6°
4°
2°
0°
−2°
6°
8°
10°
12°
14°
16°
18°

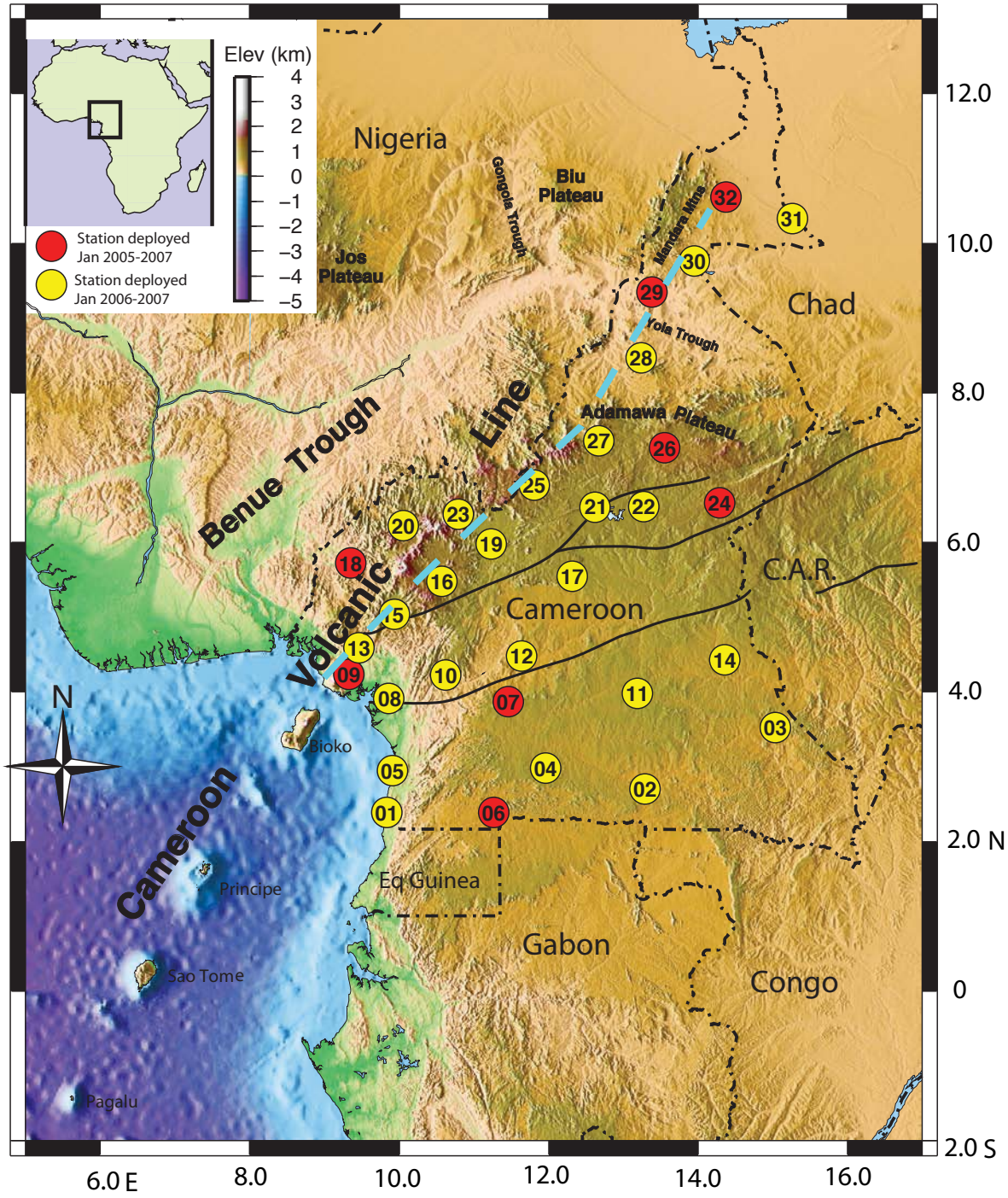
Elev (km)
4
3
2
1
0
−1
−2
−3
−4
−5
Station deployed Jan 2005-2007
Station deployed Jan 2006-2007
Nigeria
Jos Plateau
Gongola Trough
Biu Plateau
Mandara Mtns
Chad
Yola Trough
Adamawa Plateau
Benue Trough
Volcanic Line
Cameroon
C.A.R.
Bioko
Cameroon
Principe
Sao Tome
Pagalu
Eq Guinea
Gabon
Congo
N
12.0
10.0
8.0
6.0
4.0
2.0 N
0
2.0 S
6.0 E
8.0
10.0
12.0
14.0
16.0

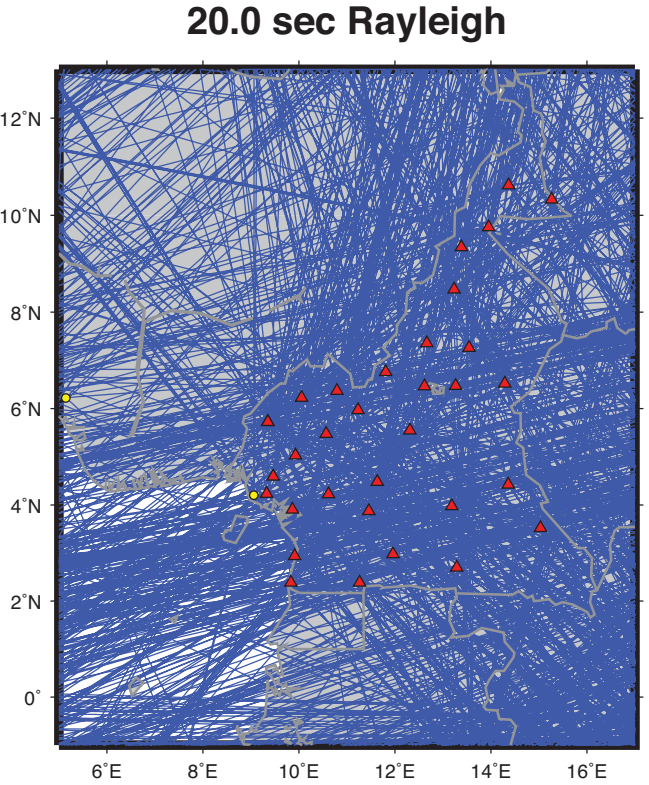
20.0 sec Rayleigh
12°N
10°N
8°N
6°N
4°N
2°N
0°
6°E
8°E
10°E
12°E
14°E
16°E

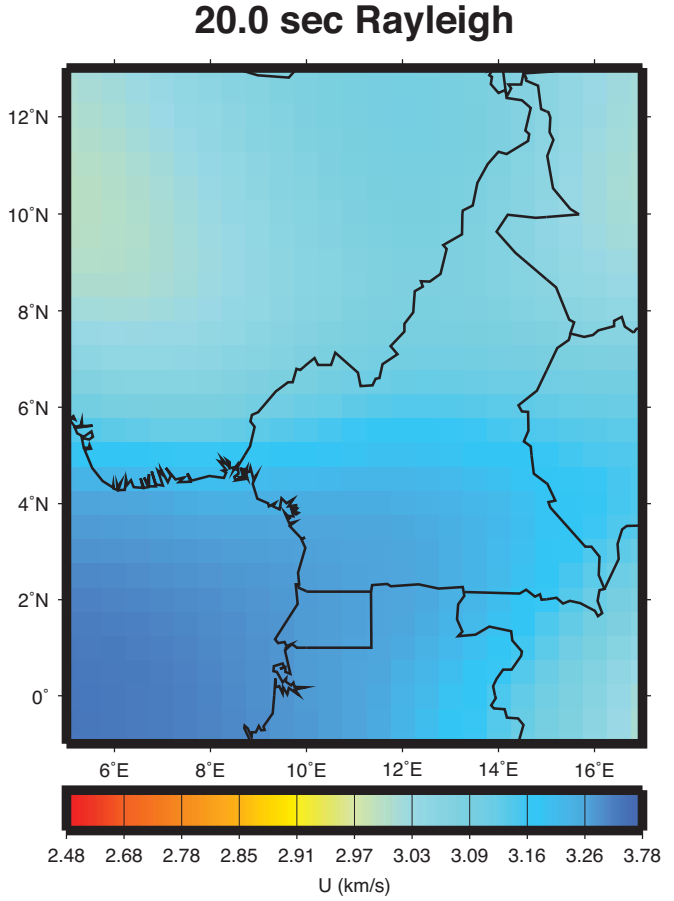
20.0 sec Rayleigh
12°N
10°N
8°N
6°N
4°N
2°N
0°
6°E
8°E
10°E
12°E
14°E
16°E
2.48 2.68 2.78 2.85 2.91 2.97 3.03 3.09 3.16 3.26 3.78
U (km/s)

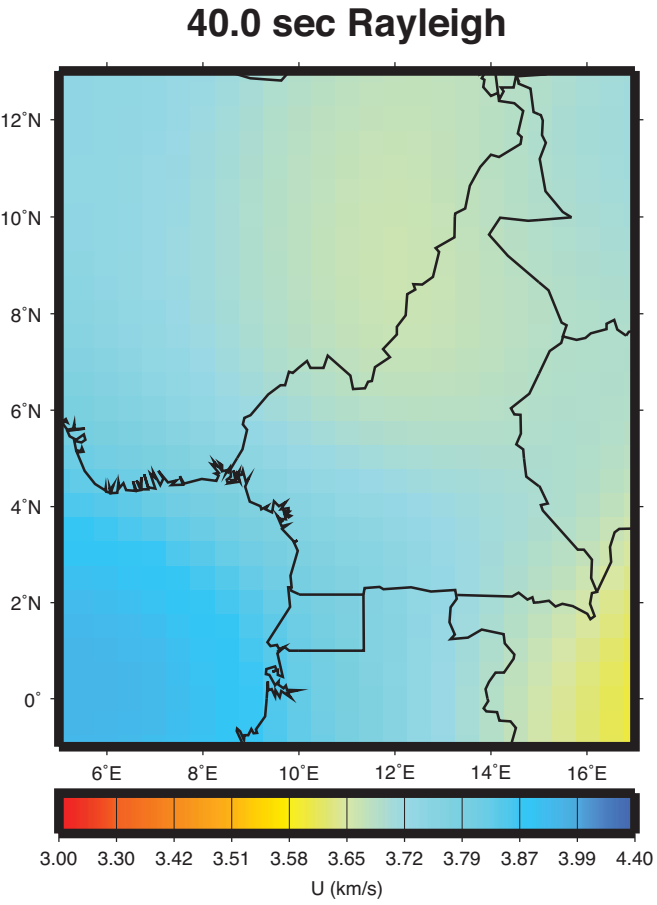
40.0 sec Rayleigh
12°N
10°N
8°N
6°N
4°N
2°N
0°
6°E
8°E
10°E
12°E
14°E
16°E
3.00 3.30 3.42 3.51 3.58 3.65 3.72 3.79 3.87 3.99 4.40
U (km/s)

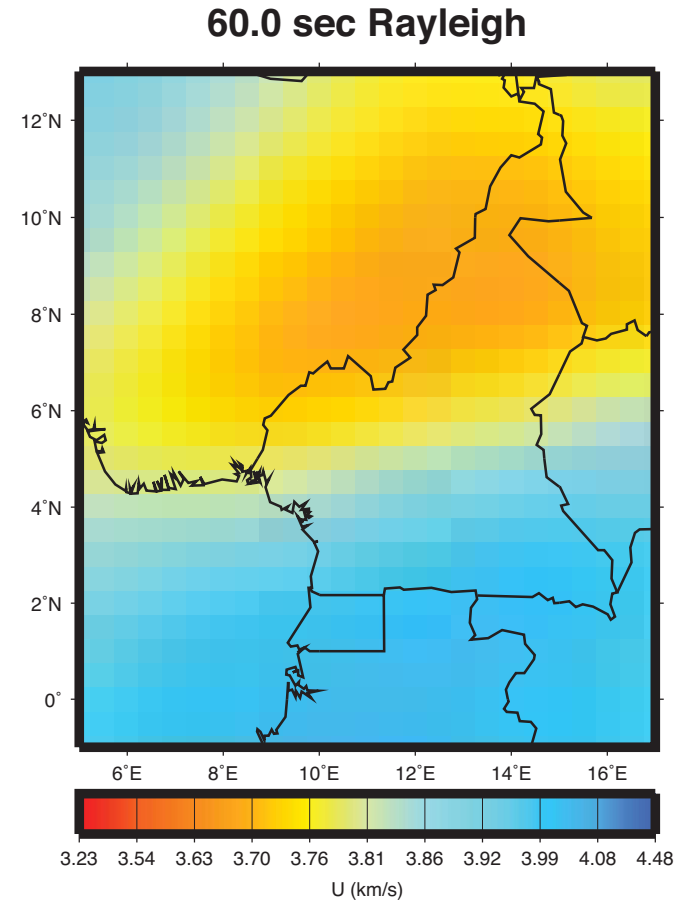
60.0 sec Rayleigh
12°N
10°N
8°N
6°N
4°N
2°N
0°
6°E
8°E
10°E
12°E
14°E
16°E
3.23 3.54 3.63 3.70 3.76 3.81 3.86 3.92 3.99 4.08 4.48
U (km/s)

Figure 4

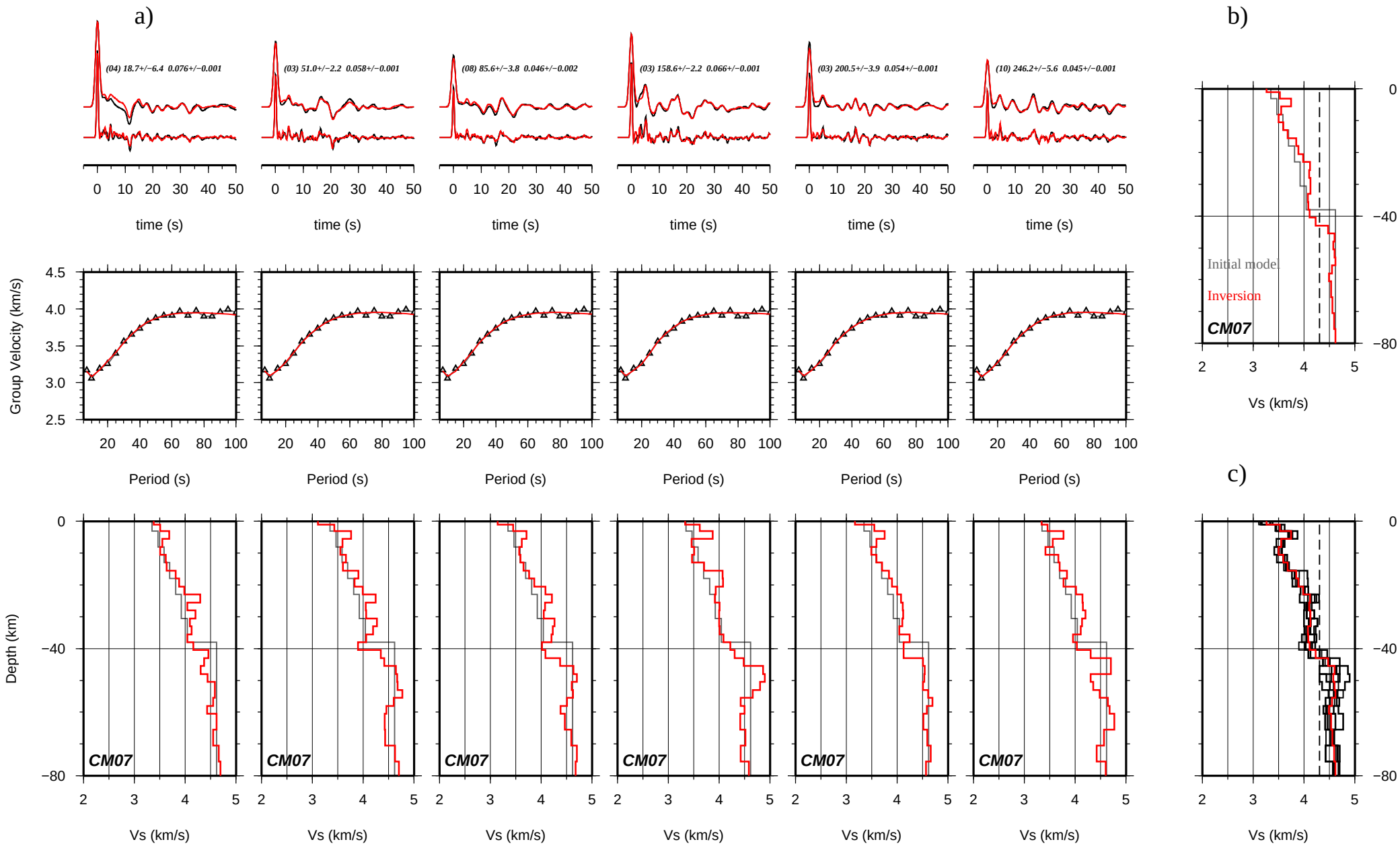
a)
(04) 18.7+/−6.4 0.076+/−0.001
(03) 51.0+/−2.2 0.058+/−0.001
(08) 85.6+/−3.8 0.046+/−0.002
(03) 158.6+/−2.2 0.066+/−0.001
(03) 200.5+/−3.9 0.054+/−0.001
(10) 246.2+/−5.6 0.045+/−0.001
time (s)
Group Velocity (km/s)
Period (s)
Depth (km)
Vs (km/s)
CM07
b)
Initial model
Inversion
c)

Figure 5

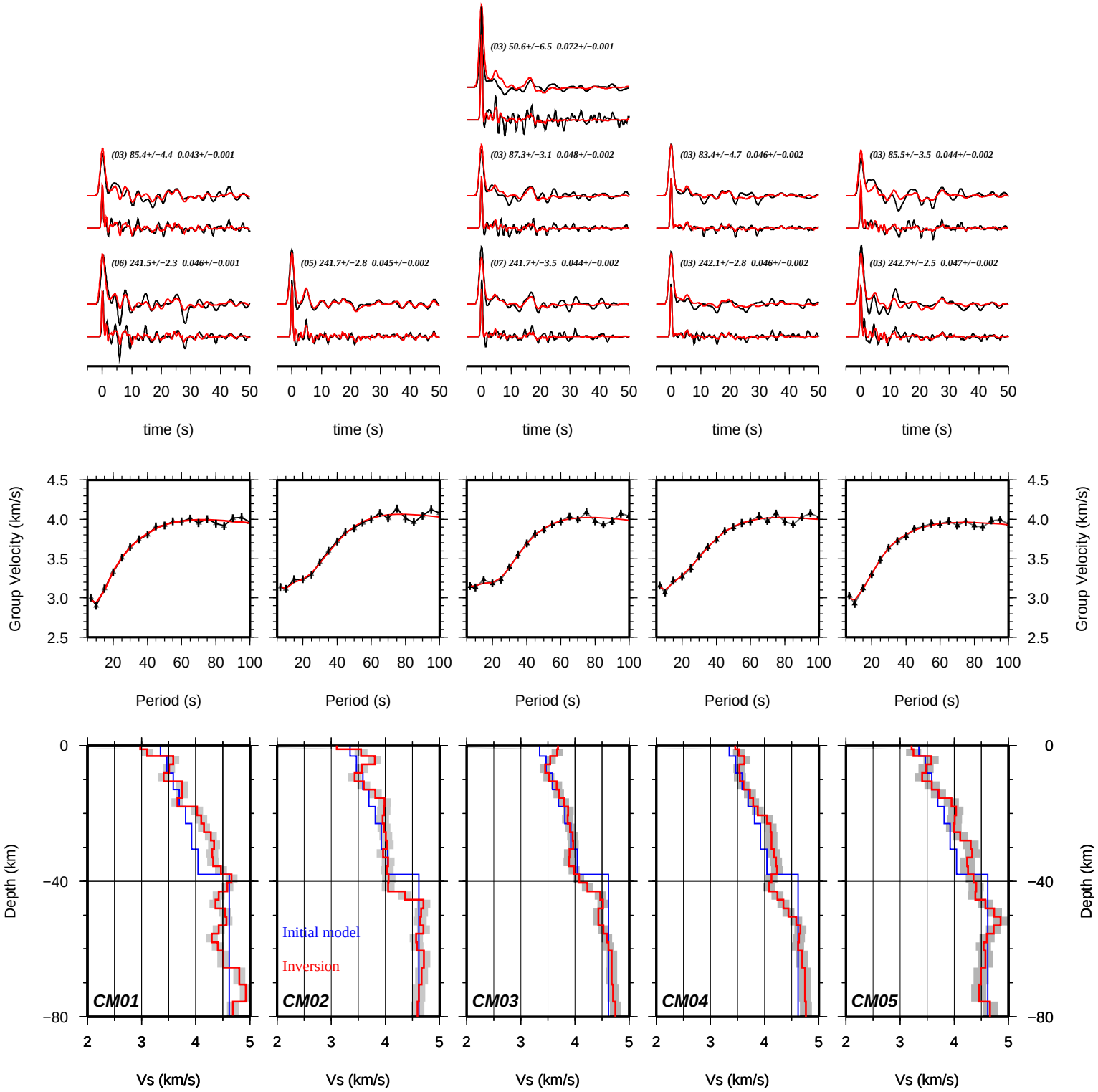
(03) 50.6+/−6.5 0.072+/−0.001
(03) 85.4+/−4.4 0.043+/−0.001
(03) 87.3+/−3.1 0.048+/−0.002
(03) 83.4+/−4.7 0.046+/−0.002
(03) 85.5+/−3.5 0.044+/−0.002
(06) 241.5+/−2.3 0.046+/−0.001
(05) 241.7+/−2.8 0.045+/−0.002
(07) 241.7+/−3.5 0.044+/−0.002
(03) 242.1+/−2.8 0.046+/−0.002
(03) 242.7+/−2.5 0.047+/−0.002
time (s)
Group Velocity (km/s)
Period (s)
Depth (km)
Vs (km/s)
Initial model
Inversion
CM01
CM02
CM03
CM04
CM05

Figure 5 continued

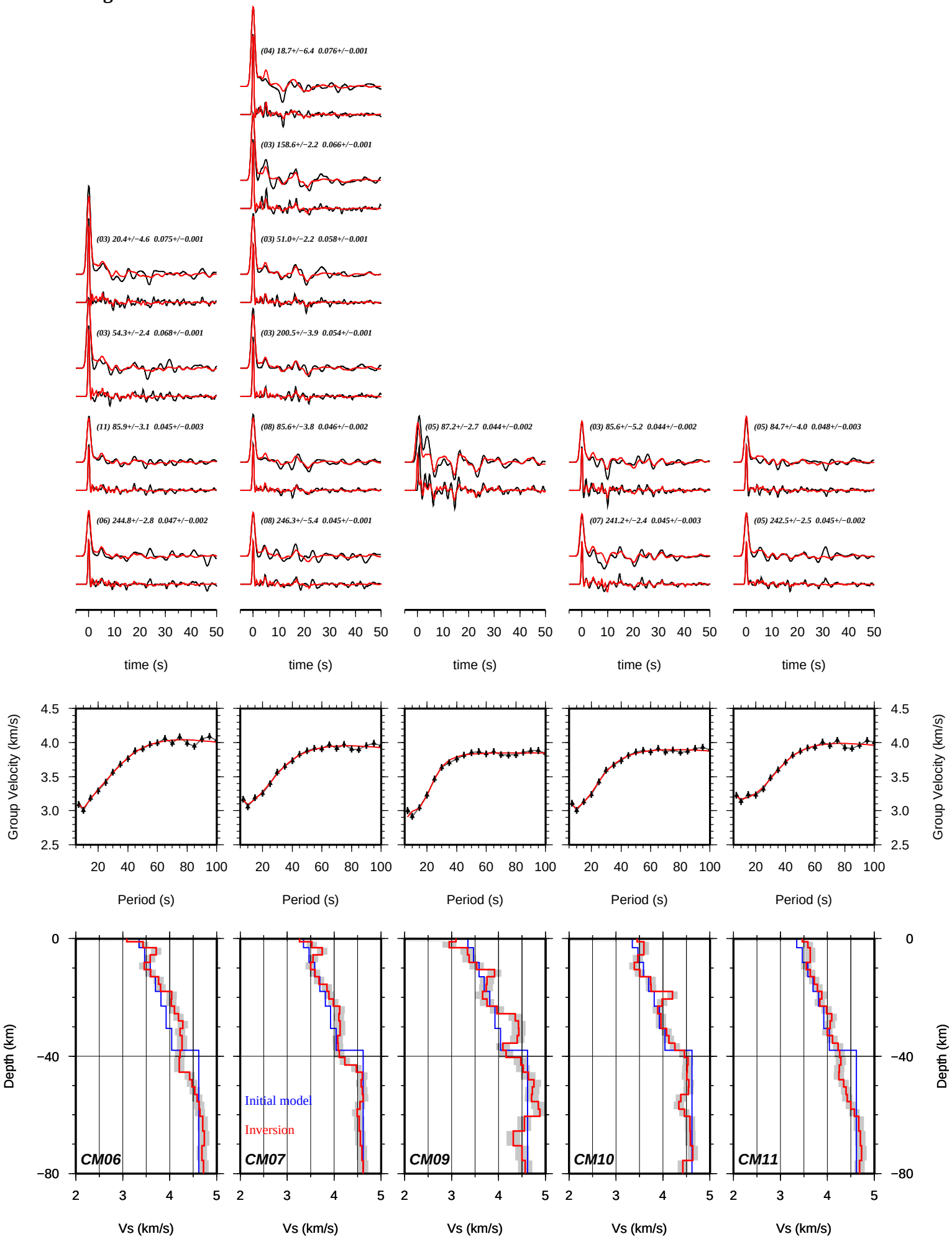

Figure 5 continued

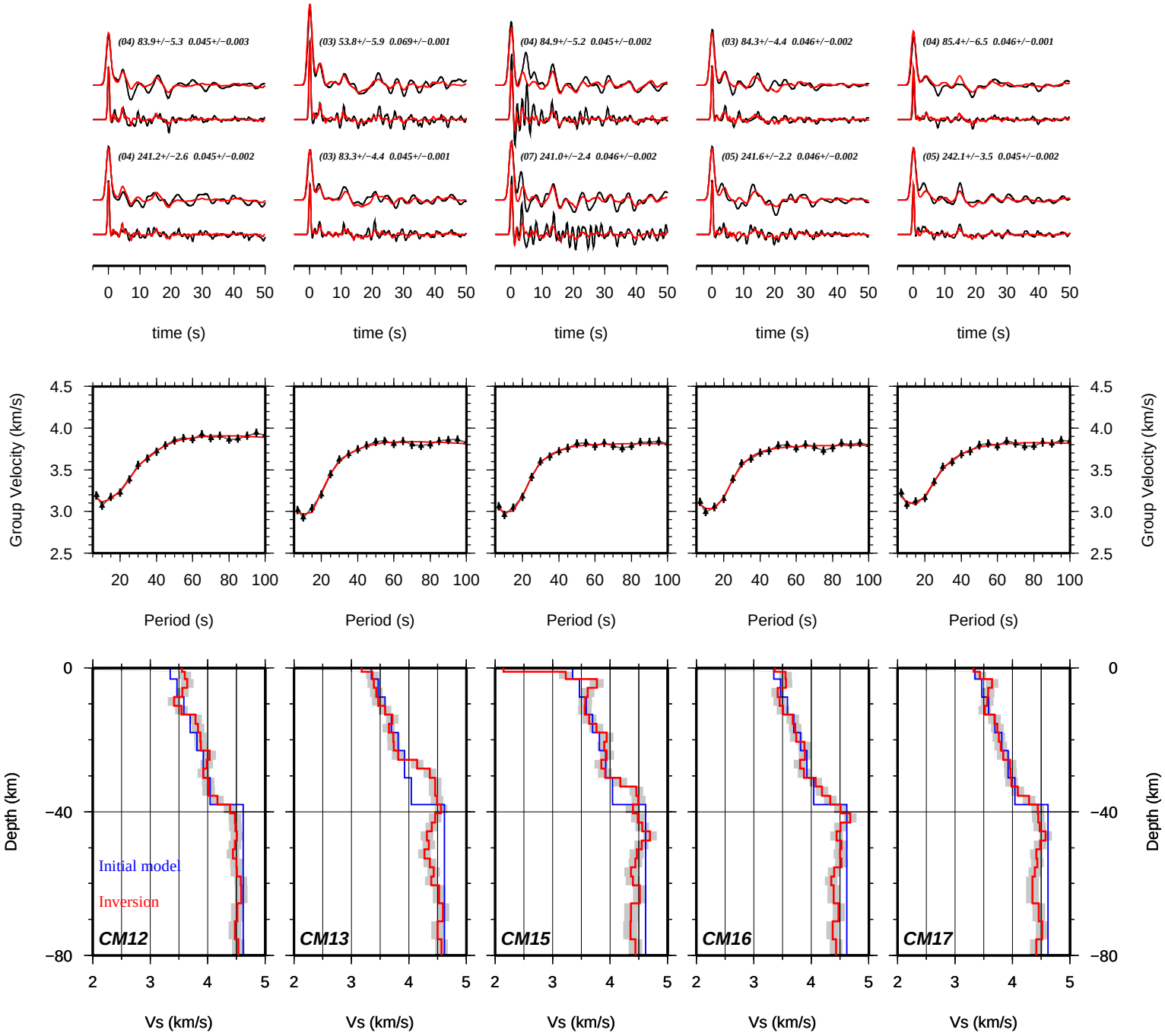

Figure 5 continued

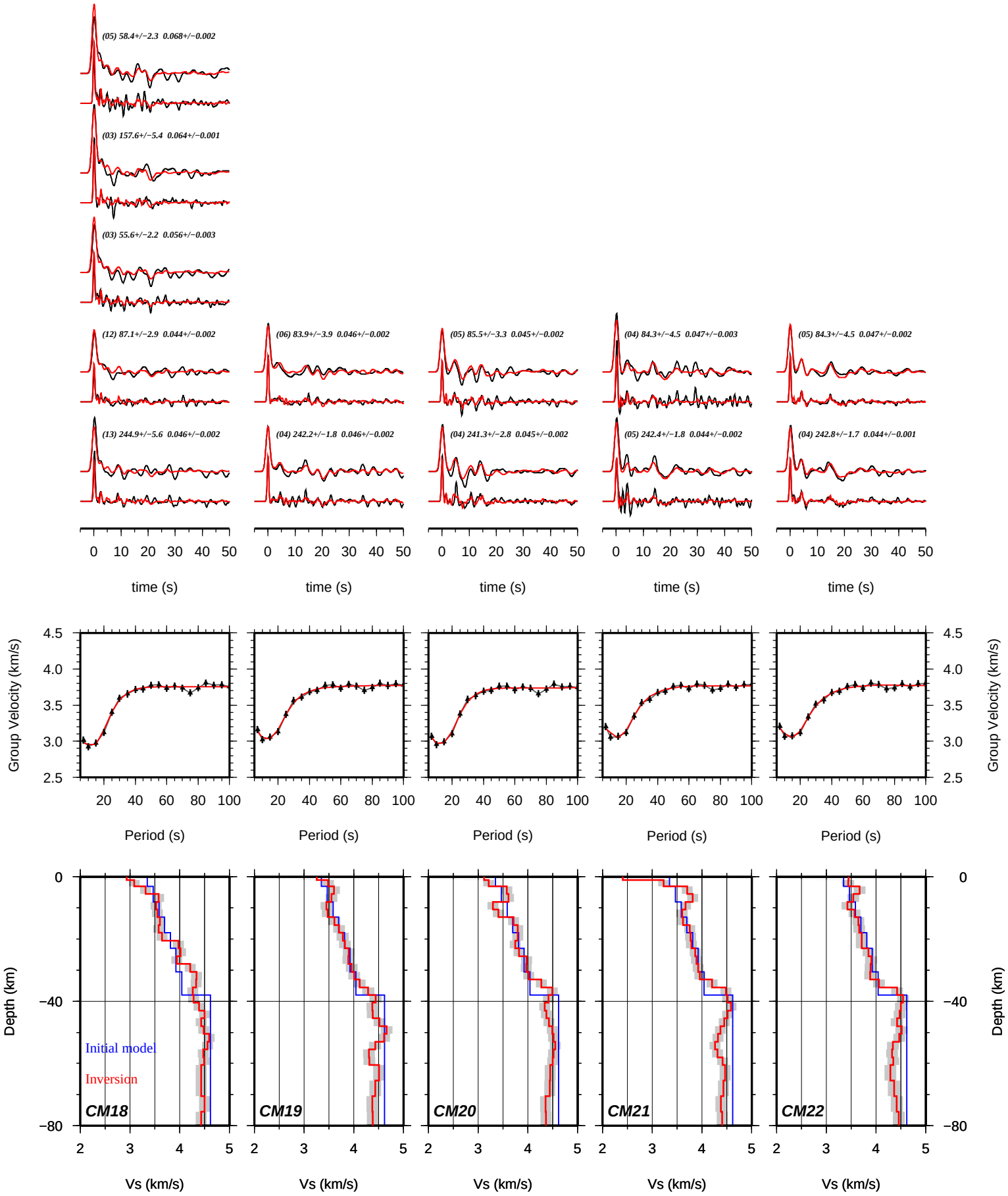

Figure 5 continued

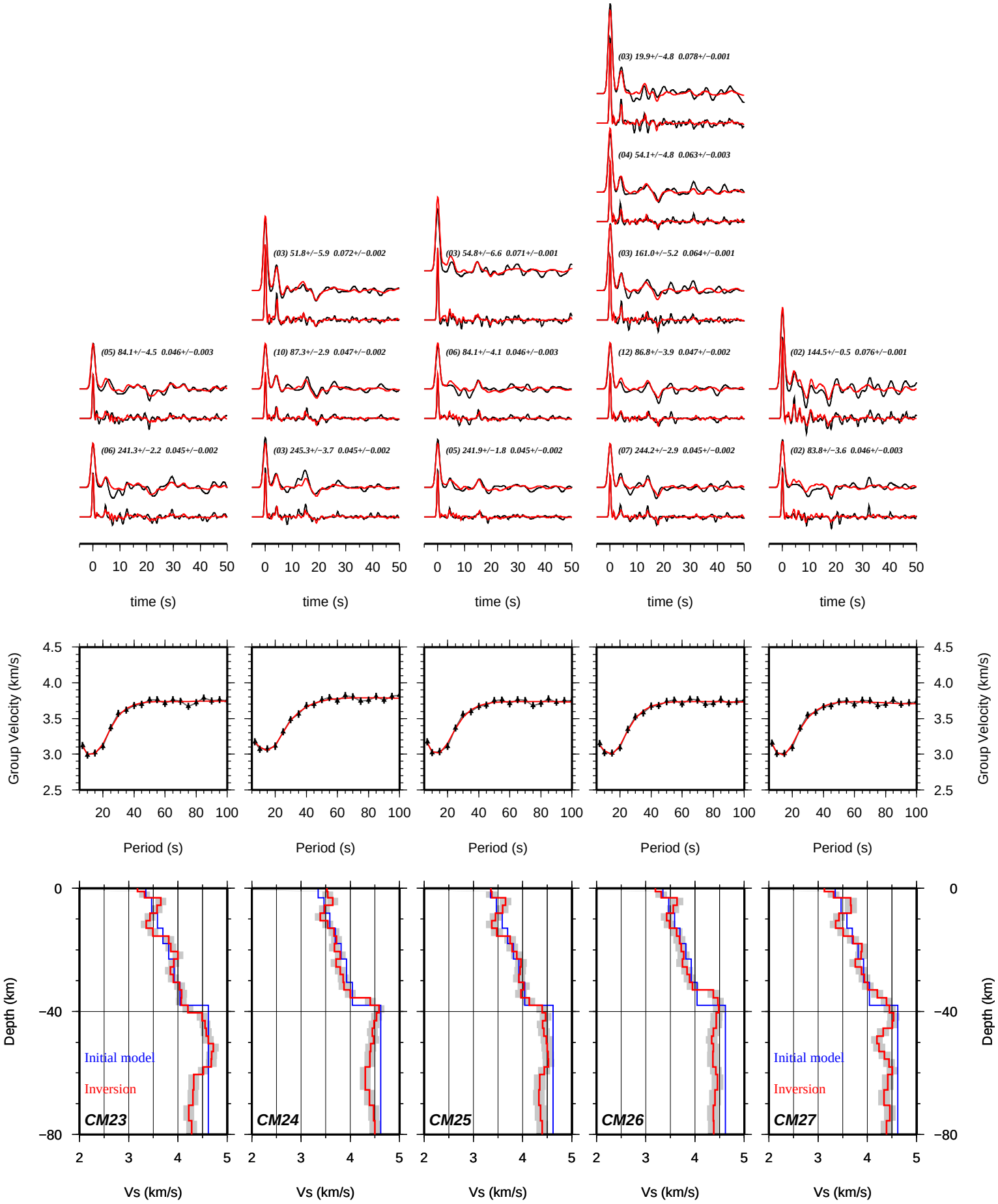

Figure 5 continued

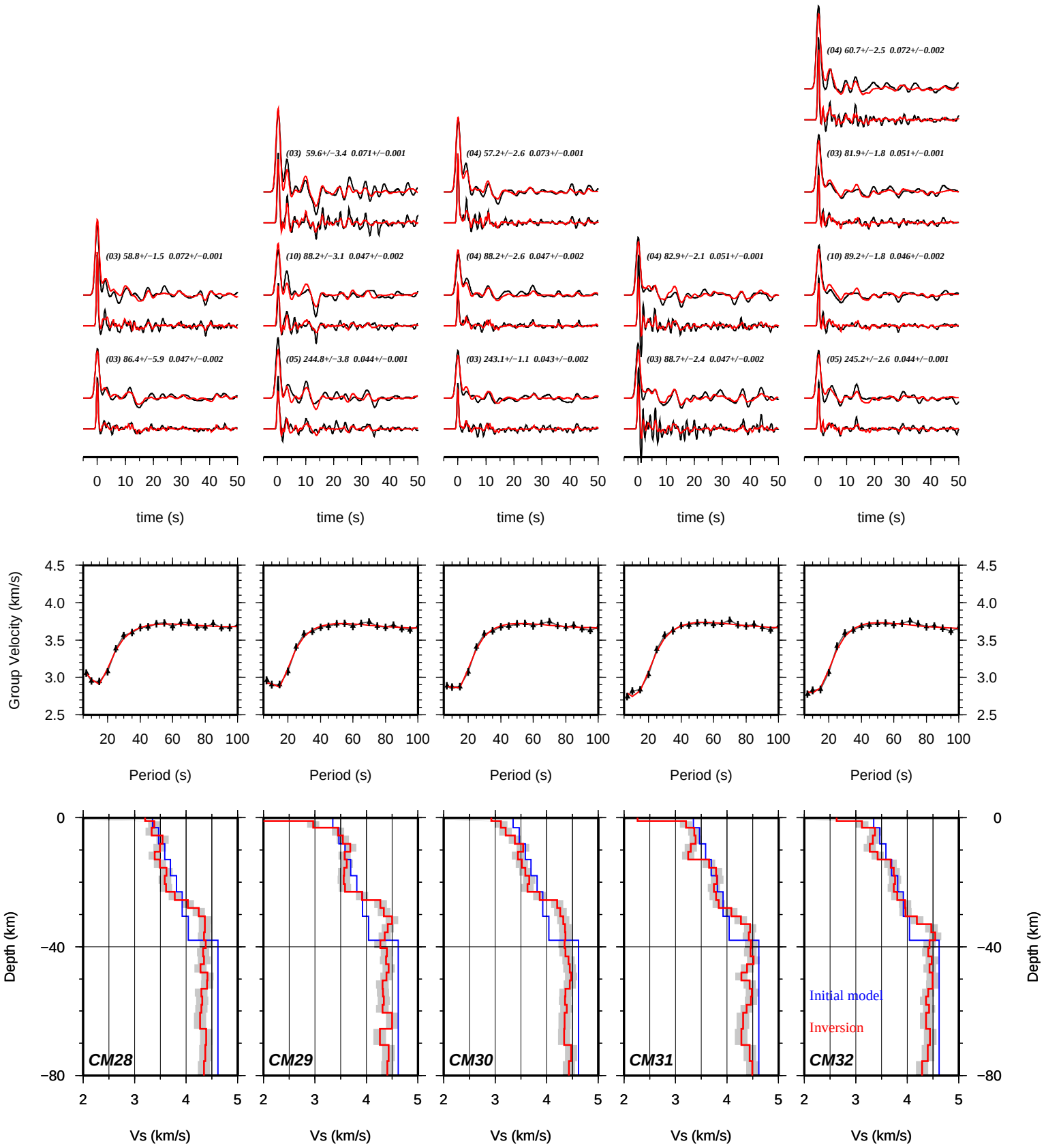

Figure 6

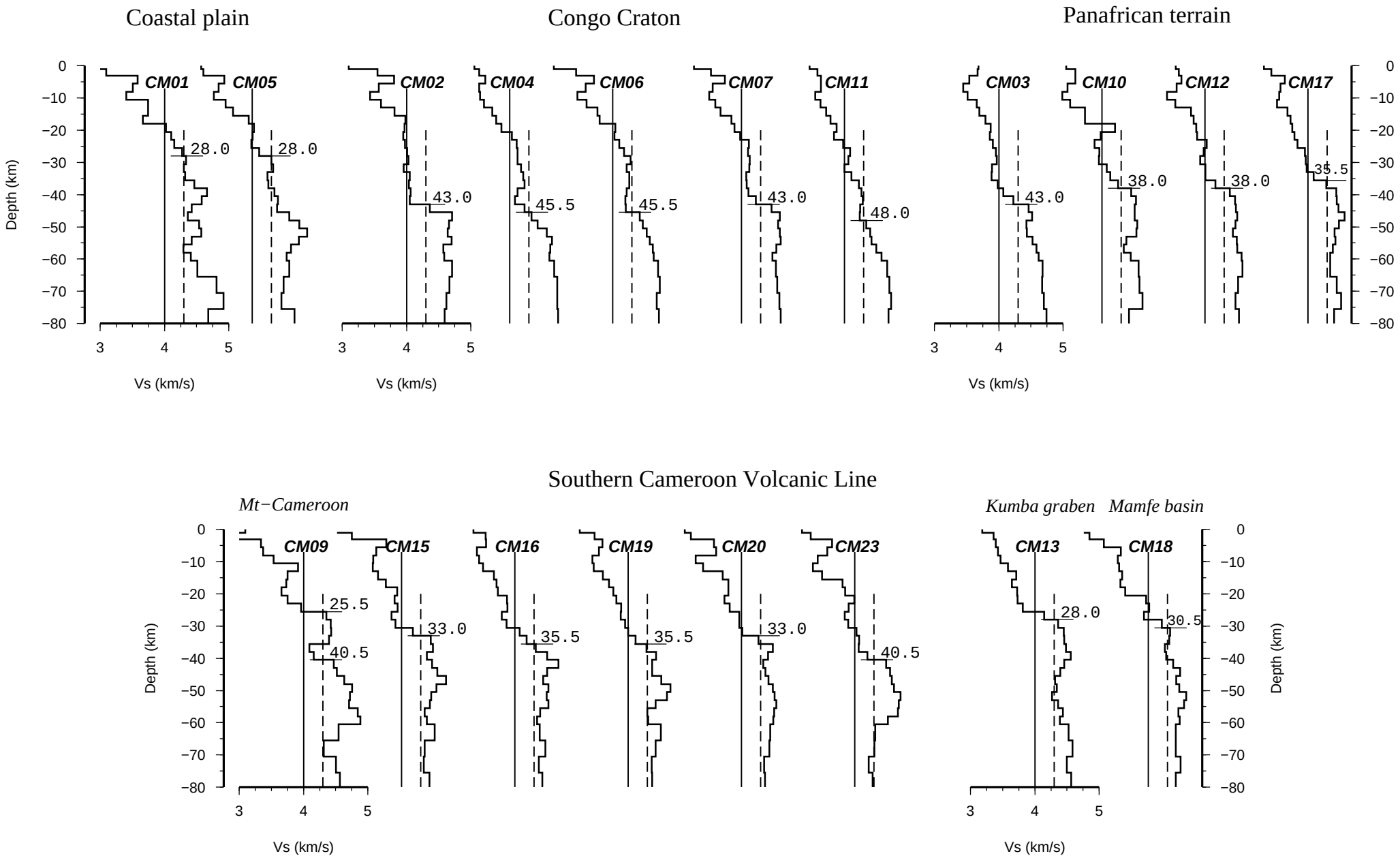
Coastal plain
Congo Craton
Panafrican terrain
Southern Cameroon Volcanic Line
Mt−Cameroon
Kumba graben
Mamfe basin
CM01
CM05
CM02
CM04
CM06
CM07
CM11
CM03
CM10
CM12
CM17
CM09
CM15
CM16
CM19
CM20
CM23
CM13
CM18
28.0
28.0
43.0
45.5
45.5
43.0
48.0
43.0
38.0
38.0
35.5
25.5
40.5
33.0
35.5
35.5
33.0
40.5
28.0
30.5
Depth (km)
Vs (km/s)
0
−10
−20
−30
−40
−50
−60
−70
−80
3
4
5

Figure 6 continued

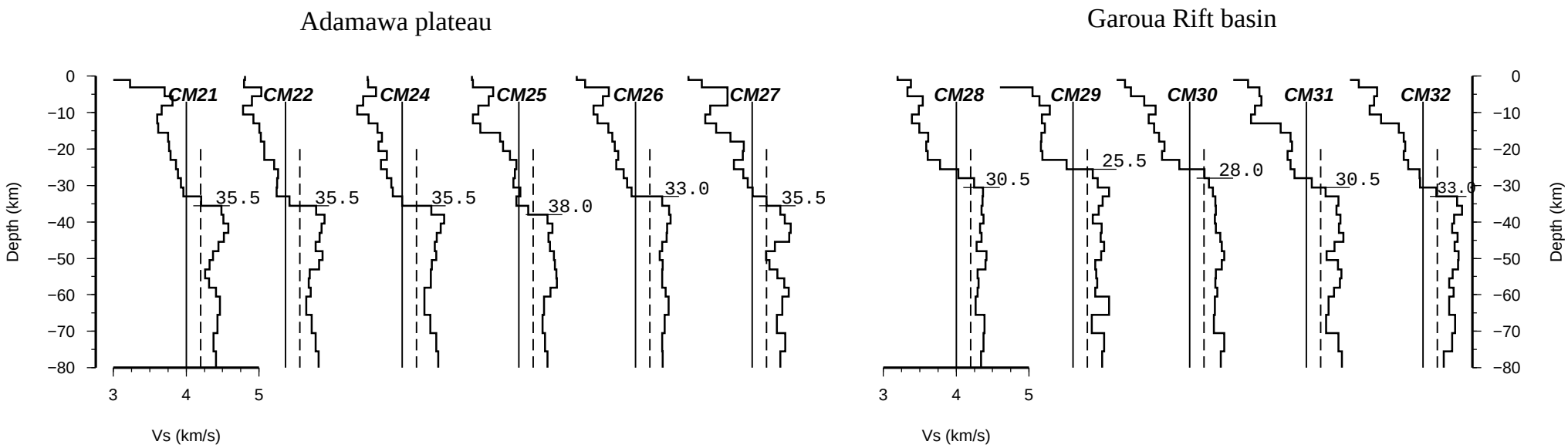

Figure 7

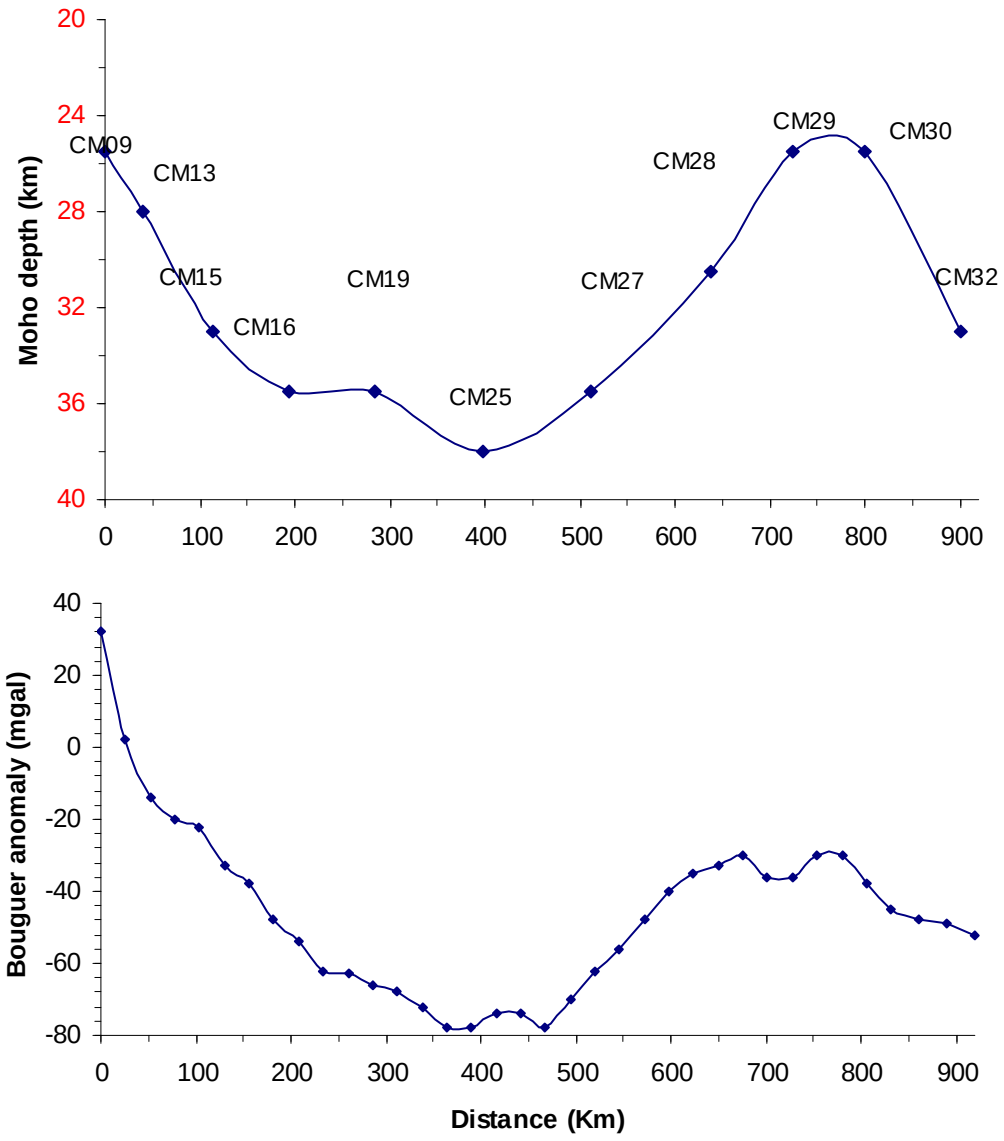
Moho depth (km)
20
24
28
32
36
40
CM09
CM13
CM15
CM16
CM19
CM25
CM27
CM28
CM29
CM30
CM32
0
100
200
300
400
500
600
700
800
900
Bouguer anomaly (mgal)
40
20
0
-20
-40
-60
-80
Distance (Km)